Division of Pharmaceutical Chemistry and Technology
Faculty of Pharmacy
University of Helsinki
Finland

Modern analytical approaches to pharmaceutical powder characterisation and processing

Ira Soppela

ACADEMIC DISSERTATION

To be presented, with the permission of the Faculty of Pharmacy of the University of Helsinki, for public examination in lecture room 2, B building, Latokartanonkaari 7, on the 24th April 2015, at 12 noon.

Helsinki 2015

Supervisors	Professor Jouko Yliruusi Pharmaceutical technology Faculty of Pharmacy University of Helsinki Finland
	Professor Niklas Sandler Pharmaceutical Sciences Laboratory Department of Biosciences Abo Akademi University Finland
Reviewers	Doctor Karin Kogermann Department of Pharmacy Faculty of Medicine University of Tartu Estonia
	Doctor Sanni Matero Novartis AG Basel Switzerland
Opponent	Professor Thomas De Beer Laboratory of Pharmaceutical Process Analytical Technology Faculty of Pharmaceutical Sciences Ghent University Belgium

ISBN 978-951-51-0977-4 (pbk.)
ISBN 978-951-51-0978-1 (PDF, http://ethesis.helsinki.fi)

Unigrafia
Helsinki 2015

Abstract

The manufacturing of the most common pharmaceutical dosage form, tablets, requires good mass flowability and uniform particle size distribution. Granulation is often needed to improve these properties prior to tablet compression. Thus, rapid methods for analysing the key powder and granule properties, such as particle size, flowability and moisture content are needed. Until recently, the development and control of pharmaceutical unit operations was based on an empirical approach rather than process understanding. To be able to build quality into the products, improved understanding of materials and processing is needed. This can be reached by developing complementary automated analytical methods that are suitable for continuous on-line or in-line process monitoring.

The aim of this thesis was to investigate whether modern analytical tools can provide rapid and reliable real-time insight into powder performance during solid dosage form processing. The first study evaluated the impact of paracetamol loading and the physical characteristics of powders on the flowability of microcrystalline cellulose and paracetamol mixtures. A novel small-scale flow device proved to be suitable for rapid flowability screening of different formulations. Particle size distribution and drug loading had the largest impact on the flowability.

The main focus of this thesis was on the utilisation of image analysis, near infrared (NIR) spectrocopy and process measurements as complementary process analytical tools during granulation. In addition to particle size distribution, the images revealed batch specific granule growth and attrition behaviour in real time. The changes in granule size were clearly linked to the continuously measured process conditions. Moreover, changes in image brightness during drying reflected the removal of water from the granules. The continuous moisture measurements based on process air moisture content and NIR spectroscopy provided real time information on the moisture content as well as the batch moisture profile during processing. The comparison of the methods also enabled the evaluation of the location of water in the process. The combination of on-line photometric imaging and near-infrared spectroscopy with continuous in-line process measurements facilitated continuous evaluation of key product properties during fluid bed granulation and provided insight into batch performance.

The powder characterisation and process analytical technology (PAT) tools applied in this work enabled rapid and non-destructive determination of key powder and granule quality attributes. Even small changes in the material properties during processing were detected using the continuous and complementary process analytical measurements.

Acknowledgements

This work was carried out at the Division of Pharmaceutical Chemistry and Technology, Faculty of Pharmacy, University of Helsinki, during the years 2009–2014.

I would like to thank my supervisor, professor Jouko Yliruusi, for giving me the possibility to work in his group and for sharing his knowledge in physical pharmacy. I wish to express my sincere gratitude to professor Niklas Sandler for his advice, support and endlessly encouraging attitude through the years. Thank you for introducing me into the world of photometric imaging, too. I am indebted to docent Osmo Antikainen particularly for his invaluable contribution to NIR data processing. I would also like to thank all my co-authors for their contributions to the work. Moreover, doctor Heikki Räikkönen's effort in fixing and maintaining the granulator is very much appreciated.

I am thankful for Doctor Karin Kogermann and Doctor Sanni Matero for reviewing this thesis and constructive comments which helped me to improve the work further.

I have been priviledged to have brilliant colleagues who together created an enjoyable and fun working environment – thank you! I would also like to thank all my friends for staying in touch despite my absent-mindedness. Siiri is especially acknowledged for all the highly creative cross-scientific chats as well as the experimental procrastibaking sessions. Siiri and Henri are also thanked for sharing some of the academic despair and frustration. Knowing that my very talented friends sometimes struggle with their research work, too, helped me to carry on at times of doubt. I would also like to extend my thanks to Hiekkisjengi for brightening my everyday life and providing peer support on managing work, hobby and family life (im)balance. I sorely miss our extemporary outdoor pancake parties already. Hélène and David, I can never thank you enough for saving me from homelessness during my first weeks in Macclesfield. If it were not for you, I would not have been able to finish this thesis on time.

I would like to thank my mother Riitta for bringing me up to be determined and independent, which are important features for a scientist. Killi and Esa, thank you for making me feel genuinely a part of your family, too. Also the countless hours of childcare are gratefully acknowledged.

Finally, I wish to express my deepest gratitude to my loved ones for the never-ending encouragement, support and putting things into perspective. Jyri, I still feel priviledged to share both the good bits and the chaos of life with you. Otso and Aarni, thank you for teaching me so much about life and and myself.

Macclesfield, March 2015

Ira

Table of contents

List of original publications

This thesis is based on the following publications:

I Soppela I, Airaksinen S, Murtomaa M, Tenho M, Hatara J, Räikkönen H, Yliruusi J, Sandler N: Investigation of the powder flow behaviour of binary mixtures of microcrystalline celluloses and paracetamol. J Excipients and Food Chem. 1(1): 55–67, 2010.

II Soppela I, Airaksinen S, Hatara J, Räikkönen H, Antikainen O, Yliruusi J, Sandler N: Rapid particle size measurement using 3D surface imaging. AAPS PharmSciTech. 12(2): 476–484, 2011.

III Soppela I, Antikainen O, Sandler N, Yliruusi J: On-line monitoring of fluid bed granulation by photometric imaging. Eur J Pharm Biopharm. 88(3): 879 – 885, 2014

IV Soppela I, Antikainen O, Sandler N, Yliruusi J: Continuous in-line and on-line moisture determination during fluid bed granulation using process data and NIR spectroscopy. Submitted

V Soppela I, Antikainen O, Sandler N, Yliruusi J: Continuous visualisation and monitoring of moisture content and particle size trends during granulation by NIR spectroscopy without the need for multivariate analysis. Manuscript

The publications are referred to in the text by their roman numerals.

Abbreviations

API	Active pharmaceutical ingredient
a_w	Water activity
AWA	Apparent water absorption
CP	Carrier payload
d_{10}	Diameter at which 10% of a sample is comprised of smaller particles
d_{50}	Diameter at which 50% of a sample is comprised of smaller particles
d_{90}	Diameter at which 90% of a sample's mass is comprised of smaller particles
d_{bulk}	Bulk density
d_{tap}	Tap density
FDA	Food and Drug Administration
FBRM	Focused beam reflectance measurement
LOD	Loss on drying
MCC	Microcrystalline cellulose
MCS	Multiple scatter correction
NIR	Near-infrared
PAT	Process analytical technology
PCA	Principal component analysis
PCR	Principal component regression
PLS	Partial least squares
PSD	Particle size distribution
PVP	Polyvinylpyrrolidone
SEM	Scanning electron microscopy
SFV	Spatial filtering velocimetry
SNV	Standard normal variate
SSA	Specific surface area
SSC	Specific surface charge
QbD	Quality by Design

1 Introduction

The manufacturing of the most widely used dosage forms, tablets, is typically preceded by other processes such as blending and granulation. Achieving the required intermediate product quality during pre-processing is of fundamental importance in terms of ensuring the end product quality. Thus, analysing the intermediate products and implementing continuous analytics to their manufacturing processes has become an important field of study during the past decade. In general, empirical approach to pharmaceutical development has made way to a more scientific approach in the recent years.

The key product properties to monitor in granulation processes are the moisture content and particle size distribution (PSD) of the product. Also the moisture profile during the process has been shown to play a role in tablettability (Hartung et al., 2011). Research in the field of PAT has been particularly active since the US Food and Drug Administration (FDA) started promoting it ten years ago (FDA, 2004). Relatively recently, the focus has expanded to Quality by Design (QbD), an approach aiming at building quality into products by systematic planning of operations based on product and process understanding (ICH, 2009). To deliver the full potential of QbD, improved understanding of materials and processing is needed. This can be reached by developing automated analytical methods that are suitable for continuous on-line or in-line monitoring of processes.

NIR spectroscopy has become the most widely studied and used PAT tool during the past decade due to its wide applicability to characterisation of both physical and chemical properties (De Beer et al., 2011, Saerens et al., 2014, Rosas et al., 2014, Otsuka et al., 2014). It is also gaining ground in process monitoring in the pharmaceutical industry (Ward et al., 2013, Wahl et al., 2014). However, the interpretation of NIR spectra can be challenging due to the combination of chemical and physical information. Thus, process analytics would benefit from complementary tools, particularly those providing direct visual information on the materials during processing. Image analysis has been widely used for particle size characterisation but the applicability of many image features, such as brightness as well as the qualitative information obtained from images have not attracted much attention.

Improved material and process understanding is also the key to successful development of robust continuous manufacturing processes tolerant to variation. The aspiration of the pharmaceutical industry to move towards automated and continuous processes requires rapid, representative and automatable PAT tools which do not disturb the manufacturing process.

2 Review of the literature

2.1 Pharmaceutical powders

Powders are the most common starting materials in pharmaceutical manufacturing. Pharmaceutical powders include both active pharmaceutical ingredients (API) and excipients. The variety of the physico-chemical properties of different API and excipients is enormous and the powder properties play a key role in manufacturability and quality of solid dosage forms (Table 1). To improve flowability and minimize segregation, powders typically need to undergo granulation before tableting.

Table 1. *Connection between powder properties and processing and product quality attributes (modified from Hlinak et al., 2006).*

Property	Blending	Flowability	Wetting	Drying	Mechanical	Dissolution
Particle size distribution	x	x	x	x	x	x
Particle shape distribution		x				
Density		x	x		x	
Surface area	x	x	x	x	x	x
Surface energy	x	x	x			
Pore size distribution			x	x		x
Static charge	x	x				
Amorphous content			x			
Hygroscopicity		x		x		

2.1.1 Particle size and shape

Particle size is among the most important particle properties affecting practically the whole manufacturing process: mixing (Swaminathan and Kildsig, 2002), granulation (Shiraishi et al., 1995) and tableting (Yajima et al., 1996, Sun and Grant, 2001). Typical median granule size in tableting is 350–700 μm (Armstrong, 1997). Since the particle size of the vast majority of APIs and excipients is significantly smaller than this and the particles have varying morphology, granulation is typically needed.

2.1.2 Flowability

Flowability is affected by both particle and inter-particle properties (Staniforth, 2007, Teunou et al., 1999). These include the physical properties of the powder, such as particle size, shape and size distribution. Particles larger than 200–250 μm usually flow freely while fine particles smaller than 100 μm are generally prone to poor flowability due to cohesion. Moreover, narrow PSD improves flowability (Liu et al., 2008) and decreases segregation (Gauthier et al., 1999). The interparticle adhesion is influenced by the particle surface properties such as texture, surface chemistry, adsorption layers, and contact area (Karra and Fuerstenau, 1977, Bailey, 1984, Visser, 1989, Zeng et al., 2000, Li et al., 2004). These properties affect intermolecular forces, such as van der Waals forces, local chemical bonds, electrostatic charges, and bridging forces and surface liquid capillary attractions (Li et al., 2004, Hassan and Lau, 2009). Depending on the material, moisture can either improve or, more often, deteriorate flowability (Crouter and Briens, 2014, Faqih et al., 2007, Teunou et al., 1999).

Different methods are typically needed to characterise different aspects of powder flowability (Krantz et al., 2009). Due to the large number of factors influencing the flow rate of a powder, only a few direct methods for measuring flowability of powders have been developed (Crowder and Hickey, 1999, Jiang et al., 2009, Ruppel et al., 2009).

2.1.3 Moisture content and wetting

Powder moisture content also plays a role during solid dosage form manufacturing. The water sorption mechanism into the solid is defined by the crystal and porous structure, water-solubility and the ability to form crystal hydrates (Dawoodbhai and Rhodes, 1989). The water sorption and desorption behaviour of a material is described by water sorption isotherms at constant temperature (Labuza, 1968). The equilibrium moisture content at a given relative humidity and temperature is the moisture content at which water sorption or desorption is absent. The equilibrium moisture content describes maximum water sorption capacity of a material.

Four types of interaction between water and crystalline solids exist: 1) adsorption on the particle surfaces, 2) capillary condensation to the microporous regions, 3) crystal hydrate formation and 4) deliquescence (Zografi, 1988, Ahlneck and Zografi, 1990). The ability of the water to enter and leave the crystal unit cell depends on the stoichiometry, position of the water molecules and the interaction strength. Porous amorphous or partially amorphous materials are typically capable of absorbing and releasing large amounts of water, which can be located either inside the particles between fibres or outside, condensed in capillaries or adsorbed to surface.

2.2 Fluid bed granulation

The most commonly used pharmaceutical wet granulation methods are fluid bed granulation and high shear granulation with subsequent fluid bed drying (Schaefer, 1988,

Wørts, 1998). Fluid bed granulation consists of mixing, liquid addition and drying and is a complex process influenced by formulation, equipment and process parameters (Parikh, 2009). However, if all the variables can be controlled, fluid bed processes provide a rapid single-unit method for transforming powders into a form that better meets the needs of the next manufacturing steps. Fluid bed granulation enables good drug content uniformity at low drug concentrations, as well as control of product bulk density (d_{bulk}) and ultimately compactibility (Faure et al., 2001).

2.2.1 Granule formation

Granule formation includes three consecutive and partly overlapping phenomena: 1) wetting and nucleation, 2) consolidation and growth and 3) breakage and attrition (Ennis and Litster, 1997, Iveson et al., 2001, Bouffard et al., 2005). Collisions and coalescence of the surface-wetted particles lead to nucleation and granule growth through liquid bridge formation (Figure 1). Breakage and attrition occur especially when liquid is removed from the granules during drying. When studying the phenomena occurring during fluid bed granulation, the process is typically divided into two thermodynamically distinct stages: liquid spraying and drying.

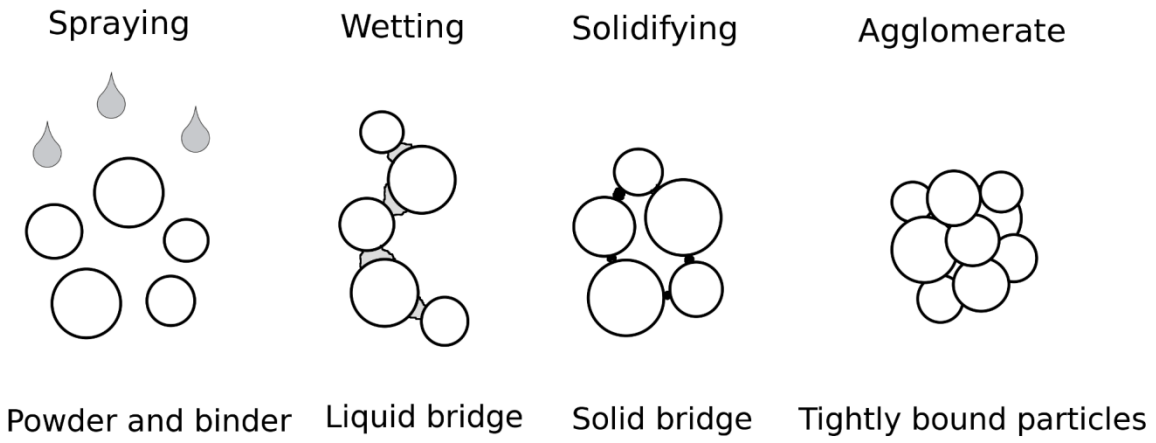

Figure 1. *Formation of granules during fluid bed granulation.*

2.2.2 Process parameters

Numerous process parameters play an important role in fluid bed granulation affecting granule size and size distribution (Table 2) (Parikh, 2009). Many of the parameters are interdependent, making full control of fluid bed granulation challenging. Higher inlet air humidity and liquid spraying rate increase median granule size by promoting liquid bridge formation (Davies and Gloor, 1971, Schaefer and Wørts, 1978, Schaafsma et al., 2000, Faure et al., 2001). By contrast, higher inlet air temperature and flow rate typically limit growth through increased surface drying (Lipps and Sakr, 1994, Rambali et al., 2001). Higher nozzle atomisation pressure produces smaller binder droplets and hence leads to

smaller granules with narrower PSD (Merkku et al., 1993, Juslin et al., 1995a, Juslin et al., 1995b, Yu et al., 1998, Hemati et al., 2003, Bouffard et al., 2005).

Table 2. *Key material, process and equipment variables affecting granule quality in top-spray fluid bed granulation (modified from Burggraeve et al., 2013).*

Starting material	Granulation liquid	Process parameter	Equipment
Particle size and size distribution	Binder type	Inlet air humidity	Nozzle position
Particle shape	Binder concentration	Inlet air temperature	Nozzle type and number of spray heads
Wettability	Viscosity	Inlet air volume	Air distributor plate design
Moisture content	Solvent	Liquid spray rate	Bowl shape
Cohesiveness		Nozzle atomisation pressure	
		Mass temperature	
		Drying time	

2.2.3 Material properties

The interaction between water and solid plays a key role in the granulation, wetting and drying behaviour of different materials. Some of the preferred starting material properties include small particle size, narrow size distribution, low density, spherical shape, minimal cohesiveness and stickiness (Parikh, 2009). Good wettability also promotes granule formation by enabling liquid bridge formation between particles (Faure et al., 2001). The solubilisation of the starting material in the granulation liquid induces granule growth. Water absorption and liquid bridge formation near the critical relative humidity is rapid (Kirsch et al., 2011). In these conditions, the thickness of the adsorbed liquid layers is sufficient (Schaafsma et al., 1999). Moreover, time-dependent mass transfer from the material to the liquid bridge solidifies the bridge. Granule growth occurs until the wetting saturation is reached and the amount of binder liquid at the agglomerate surface becomes too low for forming new liquid bridges (Schaafsma et al., 1998).

Porosity of the starting material, e.g. starch and cellulose, also greatly influences granulation through decreasing the free surface water amount (Schaafsma et al., 1998). Hence, more liquid is needed when absorbing materials are granulated (Schaefer and Worts, 1977, Schinzinger and Schmidt, 2005).

The binder properties, including viscosity and concentration, type and amount also has an impact on the final product properties (Davies and Gloor, 1972, Faure et al., 2001, Rohera and Zahir, 1993, Alkan and Yuksel, 1986). An increase in viscosity typically produces larger granules resulting in increased agglomerates. The optimal binder type and amount depends on the formulation. The initial wetting conditions determine the granule

size distribution (Faure et al., 2001). The wetting conditions depend on the surface roughness and area of the solid, particle porosity and powder packing.

2.2.4 Drying

Drying includes heat transfer to the granules to remove moisture and moisture mass transfer as vapour into the surrounding gas (Parikh, 2009). Drying rate depends on the factors influencing heat and mass transfer. Free moisture content is the amount of liquid that can be readily evaporated in specified conditions. The equilibrium moisture content is the liquid amount that cannot be removed from the product in the same conditions. Fluid bed drying is a very rapid process due to the product being suspended in hot air. The drying rate depends primarily on drying capacity of the inlet air, ie. its relative humidity, temperature and flow rate (Faure et al., 2001).

Water removal during fluid bed drying is characterised by three consecutive phases (Figure 2) (Parikh, 2009). First, the mass temperature increases to approximately the wet bulb temperature of the surrounding air, which then remains constant until all surface water has been evaporated. Drying is finalised by a subsequent temperature increase. The earlier approaches to monitor drying and determine the drying end-point include sample weight loss on drying (LOD) and bed temperature. However, the LOD method typically requires stopping the drying process for the duration of the measument to avoid overdrying. On the other hand, controlling drying based on temperature requires prior product understanding and does not provide direct information on the moisture content of the granules. Moreover, these methods do not provide accurate information on the change in the moisture content during drying. Recent approaches to monitor the whole granule drying process utilise in-line NIR spectroscopy (Nieuwmeyer et al., 2007a, Peinado et al., 2011). However, acquiring spectra from moving powders posed challenge to appropriate data pre-processing and evaluation of measurement repeatability. Moreover, the major water peak at 1930 nm was outside the measurement range in the study by Nieuwmeyer and colleagues (2007a).

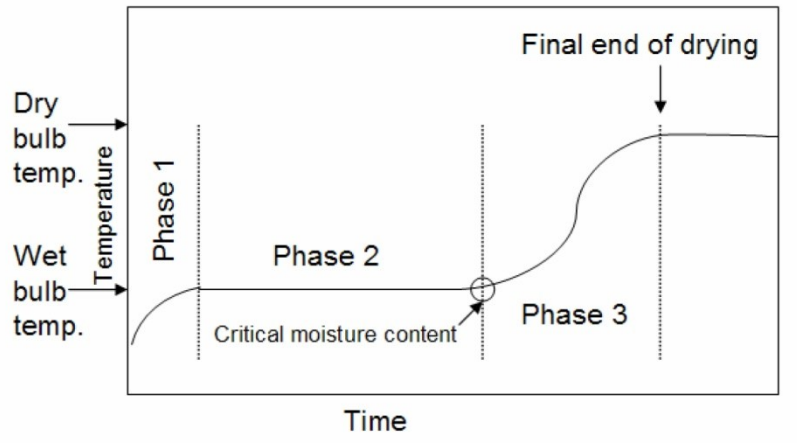

Figure 2. *Granule mass temperature profile during fluid bed drying (adapted from Parikh, 2009).*

In a successful granulation process, the liquid bridges formed between particles during the spraying phase solidify during drying (Schaafsma et al., 1998). However, insufficient liquid bridge strength leads to rapid granule attrition when solvent is removed (Nieuwmeyer et al., 2007b).

2.3 Image analysis

2.3.1 Image analysis in powder characterisation

Utilisation of direct image information in powder technology and pharmaceutical development has increased during the past two decades with the digitalisation of images, improved image resolution and computer capacity and automated data processing applications (Almeida-Prieto et al., 2006). The early applications of image information focus on the characterisation of particle size, size distribution and morphology of dispersed and stationary samples, typically by optical or scanning electron microscopy (Allen, 2003, Hellén and Yliruusi, 1993, Hellén et al., 1993). However, microscopy-based measurements from dispersed samples are time-consuming, and the challenge of representative sample preparation is a major source of error (Iacocca and German, 1997). Until rather recently, the systematic use of image information in powder technology and pharmaceutical development was rather limited apart from static and dynamic image-based particle size analysers measuring dispersed particles (Bonifazi et al., 2002, Huang and Esbensen, 2000, Eggers et al., 2008, Liao and Tarng, 2009, Wang et al., 2008). Automated dynamic image analysis has enabled the particle size measurement of a large number of particles (Besenhard et al., 2014, Patchigolla and Wilkinson, 2009, Sandler and Wilson, 2010, Yu and Hancock, 2008). Modern image-based powder characterisation methods aim at rapid measurement of a large number of particles, preferably from undispersed powders. An image-based method for measuring the PSD from undispersed granule samples was introduced by (Laitinen et al., 2004, Laitinen et al., 2002, Laitinen et al., 2003). The method was based on grey scale difference matrix (GSDM) and enabled particle size measurement from undispersed samples without sample treatment.

2.3.2 Three-dimensional images

Images reduce the three-dimensional (3D) reality into only two dimensions, resulting in loss of information on e.g. surface texture. Hence, reconstructing the 3D surface of a sample is beneficial in terms of accurate characterisation and visualisation of the morphology, particle size and surface texture (Pons et al., 1999) (Figure 3). Approaches to 3D imaging include passive triangulation methods (e.g. conventional stereo), passive photometric methods (e.g. shape from shading), active triangulation methods (e.g. structured-light) and active photometric methods such as photometric stereo (Scharstein

and Szeliski, 2002, Scharstein and Szeliski, 2003, Horn, 1970, Woodham, 1980, Lu et al., 2013, Horn and Brooks, 1989). A thorough description of the methods for 3D image reconstruction can be found in the literature (Seitz et al., 2006, Vogiatzis and Hernández, 2010, Wöhler, 2013). Recent applications of 3D surface imaging in particle size and shape analysis include on-line microscopic imaging, stereoscopic imaging and digital holography (Kempkes et al., 2010, Khanam et al., 2011, Wang et al., 2008).

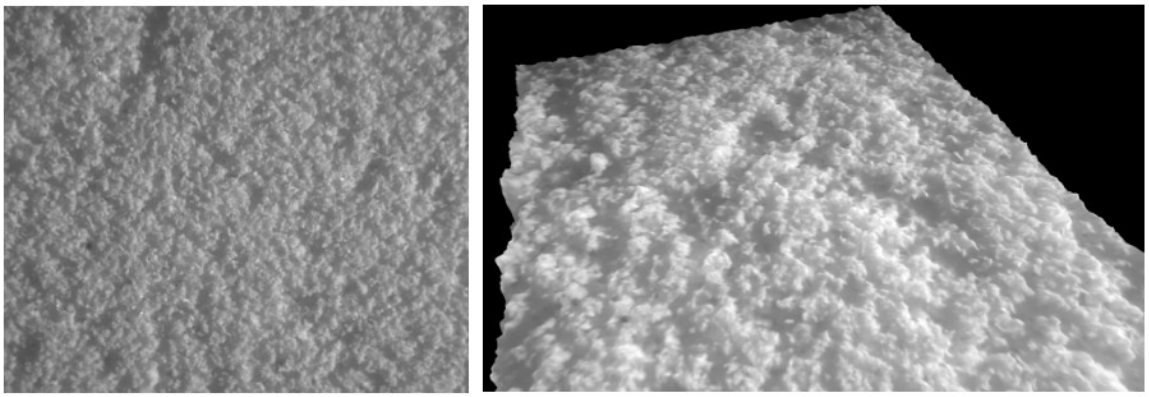

Figure 3. *Two-dimensional (left) and three-dimensional (right) images of the same granules.*

2.3.3 Photometric imaging

Photometric imaging is based on the concept of photometric stereo, which is a technique for estimating the surface normals of materials. The surface normals are obtained by varying the illumination angles (Woodham, 1980). In the photometric imaging approach, the 3D surface can be reconstructed by using different viewing angles (Russ, 2010) or with lateral illumination (Pons et al., 1999). Lateral illumination produces shades that reveal the surface texture of a sample (Figure 4). Advantages of photometric stereo include ease of identifying corresponding points in successive images due to constant viewing angle, which improves the accuracy of results. Moreover, the object shape can be described in terms of surface orientation. The photometric stereo approach has been used for measurement of the PSD of granules and pellets (Burggraeve et al., 2011a, Sandler, 2011, Fonteyne et al., 2012). In a recent study, the surface roughness of tablets measured by photometric 3D imaging was employed for the prediction of tensile strength of tablets (Halenius et al., 2014).

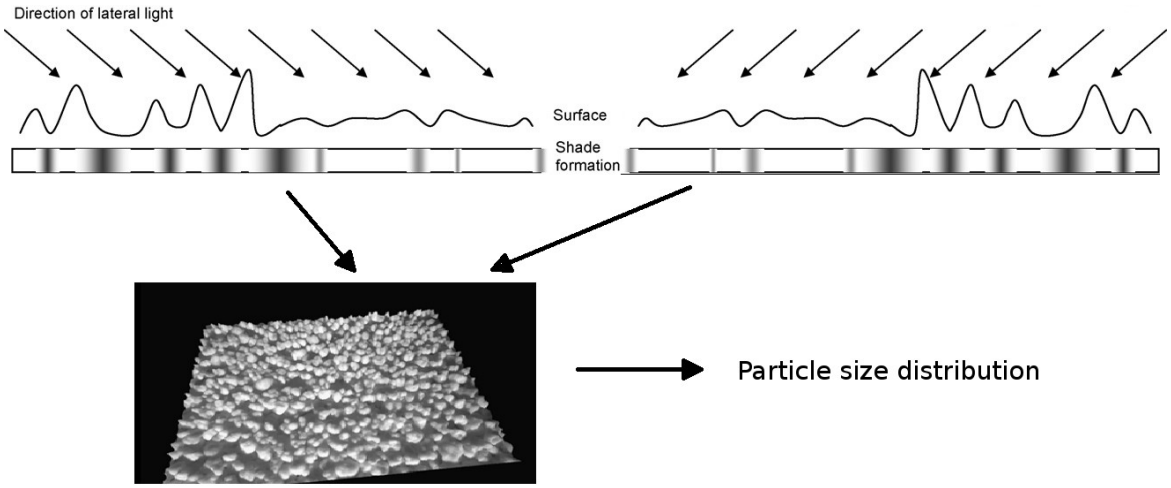

Figure 4. *Reconstruction of three-dimensionality by photometric imaging (modified from Laitinen et al., 2002).*

2.4 NIR spectroscopy

NIR spectroscopy operates at the NIR region of the electromagnetic spectrum, i.e. 780—2500 nm or 12821—4000 cm-1 (Burns and Ciurczak, 2007). Molecular absorption in these wavelengths is primarily caused by overtones and combinations of fundamental vibrations of polar groups such as O-H, N-H, S-H and C=O bonds (Siesler et al., 2008).

NIR spectroscopy follows the Lambert-Beer law (Equation 1):

$$Log\frac{I_0}{I} = A = abc \quad (1)$$

where
I_0 is the intensity of the incident light
I is the intensity measured after passing through the sample
A is absorbance
a is the absorption coefficient or the molar absorptivity
b is the path length
c is the concentration of the absorbing material

The interpretation of NIR spectra can be challenging due to the broadness of the overtone and combination bands. Moreover, NIR spectroscopy is influenced also by physical factors, such as particle size and crystallinity (Blanco et al., 1999, Blanco and Villarroya, 2002). Small particles scatter more and absorb less radiation than large particles (Barnes et al., 1989). Multivariate analysis is typically required to extract the desired chemical information. Careful selection of calibration samples and methods is important when using NIR spectroscopy.

The typical materials measured by NIR include water, carbohydrates, proteins and fats. Material identification, blending uniformity, particle size and moisture content are among the common pharmaceutical applications (Vanarase et al., 2010, Ward et al., 2013, Rantanen et al., 2001b, Fonteyne et al., 2014, Grout, 2014). NIR spectroscopy is a rapid and non-destructive technique providing both qualitative and quantitative physical and chemical information without the need for sample preparation. It is very sensitive to water and its deeper penetration depth compared to mid infrared radiation can be very useful in probing bulk materials. Due to these advantages, NIR spectroscopy is particularly useful for process analysis. The measurement depth of NIR spectroscopy depends on the wavelength, instrument settings, sample presentation and physical and chemical properties of the sample (Berntsson et al., 1998, Shi and Anderson, 2010). The penetration depth varies between 0.5–2.4 mm in powders and tablets at wavelengths 1050–1620 nm (Shi and Anderson 2010).

NIR spectrometer has to be calibrated before quantitative analysis. The calibration process typically includes 1) Selecting a representative calibration sample set, 2) Spectra acquisition and determination of reference values, 3) Multivariate modeling 4) Model validation (Reich, 2005). Chemometrics aims at producing good data through design of experiments and extracting relevant information from data through mainly multivariate data analysis (Rajalahti and Kvalheim, 2011). Pre-treatment of spectroscopic data is typically needed prior to data modelling. Pre-treatment removes irrelevant physical phenomena in the spectra and improves the data model. Choosing a pre-treatment method, which is suitable for the data set as well as the subsequent modelling step, is thus of key importance. Attention should be paid to not remove any important spectral information. The most widely used methods for NIR data pre-treatment include scatter correction and derivatives (Rinnan et al. 2009). Typical methods for reducing particle size effects are multiple scatter correction (MSC) and standard normal variate (SNV) (Dhanoa et al., 1995, Roggo et al., 2007). Also derivatives or detrending can be used for data processing (Pasikatan et al. 2001). Also appropriate data visualisation is important. Multivariate projection techniques enable sample classification, simplification of complex data and prediction of outcome and make thus visualisation easier. The most common methods are principal component analysis (PCA) and partial least-squares (PLS) regression (Jackson, 2005, Rajalahti and Kvalheim, 2011, Wold et al., 2001).

PCA is a dimension reduction technique. It transforms observations of correlated variables into a set of independent principal components. The first principal component accounts for as much of the systematic variability in the data as possible and each succeeding component contains as much of the remaining variability as possible not explained by the prior principal components. Majority of the spectral variability in pharmaceutical NIR applications can often be explained by only a few principal components. PCA has been widely used for visualising data and in qualitative analysis since it can reveal groupings, trends and outliers in the data (Reich, 2005, Rajalahti and Kvalheim, 2011). PLS is the most common method in quantitative determination of water (Luypaert et al., 2007). Moreover, the different data treatment methods for NIR spectroscopy have been described in more detail in review papers (Rajalahti and Kvalheim, 2011, Reich, 2005, Roggo et al., 2007, Rinnan et al., 2009).

2.5 Process analytical technology

The U.S. Food and Drug Administration (FDA) published a PAT guideline ten years ago to promote improved process understanding through encouraging the development of process analytical tools in pharmaceutical manufacturing (FDA, 2004). The aim is to improve the product quality through shifting the process control strategies from end product testing to real-time analyses (Figure 5). Since then, the focus has broadened to QbD introduced in the ICH Q8 guidance (ICH, 2009). QbD is an concept of building quality into products (Juran, 1992). The pharmaceutical industry is shifting from the traditional approach towards QbD. The QbD approach involves planning products and operations based on systematic and scientific product knowlegde and process understanding rather than using specifications based on empirical batch history. PAT, most typically NIR spectroscopy, can improve process understanding through providing continuous information on the material properties during processing. With appropriate process analytics, the QbD approach enables robust processes within design space that are tolerant to variation in the material and process parameters.

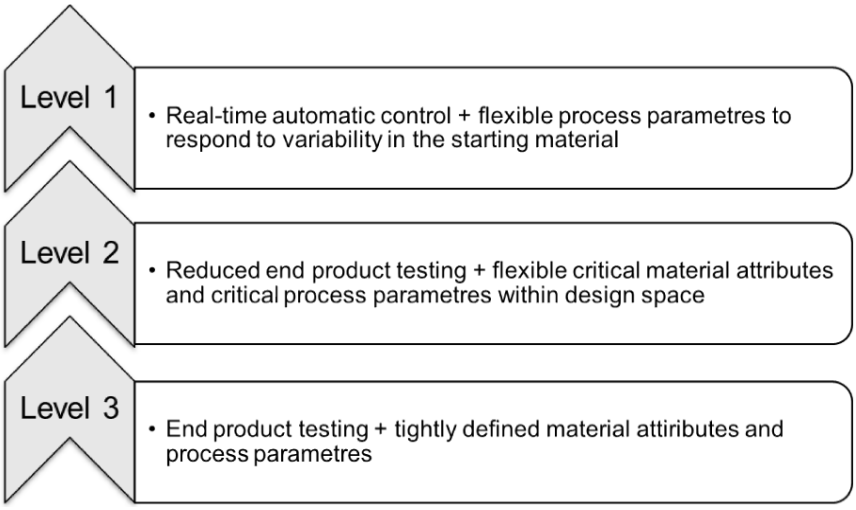

Figure 5. *Process control strategy implementation levels (modified from Lawrence et al., 2014).*

Continuous process measurements have become increasingly popular in pharmaceutical research and development. They are necessary for QbD and continuous manufacturing processes. However, moving sample and probe fouling often compromise the measurement accuracy. Moreover, probes inserted into the equipment can disturb the material movement in the process. Numerous PAT tools for monitoring pharmaceutical granulation and pelletisation processes have been developed and will be discussed in the next chapter. Process measurements can be done without collecting a sample by probing the process (in-line) (Figure 6). On-line measurements are made from samples diverted from the process stream and returned to the process after the measurement. At line measurements involve collecting samples from the process and measureing them in close proximity of the process.

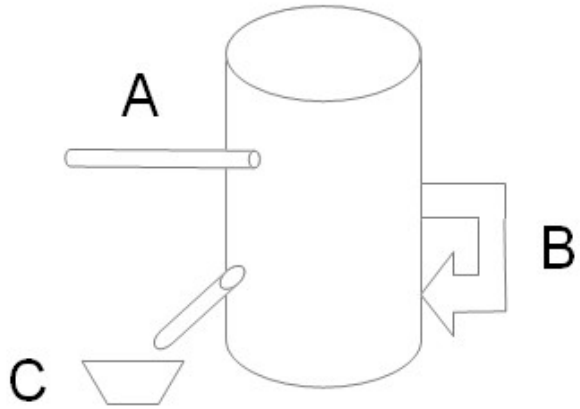

Figure 6. *Process monitoring using PAT tools A) in-line B) on-line C) at line.*

2.5.1 Traditional process measurements in fluid bed granulation

Measuring key granulation process attributes in a continuous fashion can provide valuable information on the product performance during the process. Air flow rates, relative process air humidity and temperature have been measured continuously and used for monitoring process trends earlier (Rantanen et al., 2000, Räsänen et al., 2004). Variation in the inlet air humidity has been shown to be reflected on the temperature measurements within and between batches (Lipsanen et al., 2007). A fluidisation parameter has also been defined based on the relationship of inlet airflow rate and turbine fan speed. It was able to identify risk factors and to predict process failure such as over-fluidisation, improper fluidisation and bed collapse. The authors suggested that the fluidisation parameter could be used as part of a control system to optimise the air flow rate and to evaluate if the process is within its design space.

2.5.2 Particle size and moisture content measurement during fluid bed granulation

Particle size and moisture content are the most important material quality attibutes to monitor during fluid bed granulation. They have been studied by NIR spectroscopy (Alcala et al., 2010, Findlay et al., 2005, Frake et al., 1997, Nieuwmeyer et al., 2007a, Rantanen et al., 2001b), Focused Beam Reflectance Measurement (FBRM) (Hu et al., 2008), spatial filtering velocimetry (SFV) (Petrak, 2002, Burggraeve et al., 2010, Burggraeve et al., 2011b, Närvänen et al., 2009) and acoustic emission (AE) (Halstensen and Esbensen, 2000, Halstensen et al., 2006, Halstensen and Esbensen, 2010, Matero et al., 2009, Matero et al., 2010, Matero et al., 2013, Tsujimoto et al., 2000). Also microwave resonance technology has attracted some interest (Buschmüller et al., 2008, Gradinarsky et al., 2006, Lourenço et al., 2011). However, few studies have reported continuous measurements of key quality attributes from motionless samples.

2.5.3 Image information in powder processing

Image information has been used for monitoring several powder handling processes. The first studies on using images for on-line monitoring of particle size during granulation were reported in the 90's (Watano, 2001, Watano and Miyanami, 1995, Watano et al., 1996, Watano et al., 1997). The image probe consisted of a CCD camera, optical fibers for lighting, a telephoto lens and an air purge unit. A stroboscope was used as a light source. The image-based mass median particle size and the results of sieve analysis were well in accordance, and also the shape factor of the particles was determined. These studies also showed that the position of the imaging probe has an impact on the results due to the particle segregation in fluid bed granulator. The movement of the sample, probe fouling and insufficient fluidisation close to the sampling probe typically make the in-line particle size measurements challenging. An attempt to overcome these problems and to gain direct visual information on the granulation process by measuring particle size of a static sample with an on-line or at-line surface imaging approach have also been studied (Laitinen et al., 2004, Närvänen et al., 2008, Leskinen et al., 2010, Sandler, 2011). The at-line image device used by Laitinen et al. (2004) consisted of a light source and a monochrome CCD camera with a lens objective. The particle size was calculated from the surface images based on a PLS model between the grey scale difference matrix and sieve analysis. The correlation between surface imaging and sieving was good, but the imaging device design did not allow it to be used on-line. An on-line method based on constructing a topographic image using RGB leds for illumination and a CCD camera for image capture was used for determination of the size of individual granules (Närvänen et al., 2008). The particle size trend could be calculated and the correlation to sieve analysis was fairly good. Another imaging prototype comprising a LED light source, projection optics and a CCD camera was used for on-line particle size measurement of fluidised granules (Leskinen et al., 2010). The potential applications of monochrome photometric imaging e.g. in dry milling have been described by Sandler (2011).

However, image information has been underutilised in process monitoring, focusing principally on measuring the particle size of samples either at-line or off-line. If the challenges of representative image collection can be overcome, continuously collected images can effectively visualise the behaviour of formulations through the processes. Recent advances in the utilisation of images in powder process monitoring include determination of pellet coating thickness (Kadunc et al., 2014), determination of segregation tendency of granules during tableting (Lakio et al., 2012), in-line monitoring of PSD and shape of pellets during hot-melt extrusion (Treffer et al., 2014), particle size measurement and surface characterisation (roughness and shape) of granules (Fonteyne et al., 2012).

2.5.4 Complementary PAT tools

Complementary PAT tools refer to the collection of process data using more than one PAT tool simultaneously. Complementary PAT tools can be used to maximise the information gathered from a process. Combination of complementary process analysers

can provide new information on the process or product during early development and scale-up (Burggraeve et al., 2013). The analysers need to be installed so that they provide accurate information but do not disturb the process. Well selected PAT tools can ideally monitor and control the process at production scale, maintain process robustness, and minimise process variability. Examples of complementary PAT tools for granulation processess include granulation rate monitoring by the combination of 1) acoustic emission, FBMR and NIR spectroscopy (Tok et al., 2008). Particle size and moisture content of fluid bed granules have been measured by NIR spectroscopy coupled with either SFV or FBRM (Burggraeve et al., 2012). A few studies have also used at-line image information as a complementary PAT tool for monitoring granulation (De Beer et al., 2008, Fonteyne et al., 2012). One of the very few studies utilising on-line or in-line imaging compered the particle size obtained by flash topography to acoustic emission and NIR in fluid bed granulation (Leskinen et al., 2010). Acoustic emission provided fairly precise results over a wide particle size range. Moreover, multi-point NIR and acoustic emission methods were able to differentiate between the different phases of granulation. However, the image method systematically underestimated the particle sizes by approximately 50 μm. The NIR spectra was also affected by varying particle packing. Nevertheless, the combination of images and NIR data can provide valuable real-time insight into material behaviour during powder processing. Images give direct visual information while NIR spectroscopy can capture a wide range of physico-chemical changes during the process.

3 Aims of the study

The aim of this thesis was to investigate whether modern analytical tools can provide rapid and reliable real-time insight into powder performance during solid dosage form processing. The spesific aims of the study were:

1. To study the effect of paracetamol loading and physical properties of powder blends on the flowability of paracetamol and microcrystalline cellulose (MCC) mixtures using a novel small scale flowability measurement device (I)

2. To investigate the applicability of the photometric imaging approach in particle size measurement and flow rate screening (II)

3. To study the applicability to use image information in evaluating batch performance during fluid bed granulation (III)

4. To gain insight into batch-dependent water sorption and removal kinetics in fluid bed granulation by complementary continuous in-line process measurements and on-line NIR spectroscopy (IV)

5. To visualise and evaluate particle size and moisture content changes during fluid bed granulation using a simplified data analysis approach for NIR spectroscopy (V)

6. To investigate the feasibility of photometric imaging, NIR spectroscopy and process measurements as complementary PAT tools to improve the understanding of batch performance during fluid bed granulation (III-V)

4 Materials and methods

4.1 Materials

4.1.1 Powder mixtures (I)

Altogether 48 samples consisting of paracetamol (Hawkins Inc, Minneapolis, USA) and MCCs (Avicel® PH101, PH102 or PH200, FMC BioPolymer, Little Island, Ireland) were prepared under controlled conditions (24±1°C, 50±2% RH). The paracetamol concentration ranged from 0 to 25% (w/w) with 2.5% increments.

4.1.2 Granules (II – V)

The model formulation in study II consisted of 175 g (5% w/w) of caffeine (Orion Pharma, Espoo, Finland), 475 g MCC (Emcocel 50M, Penwest Pharmaceuticals, Nastola, Finland), 2200 g lactose monohydrate (Pharmatose 200M, DMV Pharma, Veghel, The Netherlands), 500 g pregelatinised starch (Starch 1500, Colorcon, Indianapolis, IN) and 5% w/w polyvinylpyrrolidone as a binder (PVP; Kollidon K25, BASF, Ludwigshafen, Germany). Moreover, three MCCs, Avicel® PH101, PH102 and PH200 (FMC BioPolymer, Little Island, Ireland) were used as supplied.

For the papers III – V, granules consisting of paracetamol (Mallinckrodt Inc, Raleigh, NC, USA), MCC (Avicel PH101, FMC BioPolymer, Little Island, Ireland), lactose monohydrate (Pharmatose 200M, DMV Pharma, Veghel, The Netherlands) and 7% polyvinylpyrrolidone (PVP, Plasdone K25, ISP Technologies Inc, Wayne, USA) were manufactured. The drug amount was kept constant at 5% (w/w) in all formulations and the ratios of the fillers are shown in Table 3.

Table 3. *Filler proportions in the granule batches for studies III–V.*

Batch	*Lactose (%)*	*MCC (%)*
I	100	0
II	75	25
III	50	50
IV	25	75
V	0	100

4.2 Unit operations

4.2.1 Mixing (I)

The binary powder mixtures for the flowability study were mixed in 100 ml glass containers using a laboratory-scale Turbula® mixer at 22 rpm (Willy A Bachofen AG, Basel, Switzerland).

4.2.2 Granulation (II – V)

The granules studied in the paper II were manufactured with a bench-scale fluidised bed granulator (Glatt, WSG 5, Glatt Gmbh, Binzen, Germany). The batch size was 3500 g and the binder liquid contained 8.75% PVP. Depending on the batch, the inlet air temperature was between 30–50ºC, nozzle spraying pressure was 1, 1.5 or 2 bar and granulation liquid flow rate 160, 175 or 190 g/min. The flow rate of inlet air ranged from 0.04 to 0.06 m^3/s. Twenty-eight successful batches were used in this study and will be referred to as granules R1–R28. The granulation process has been thoroughly described earlier (Laitinen et al., 2004).

For the papers III–V, eight granule batches were manufactured with an instrumented bench-scale fluidised bed granulator (Glatt, WSG 5, Glatt Gmbh, Binzen, Germany). The batch size was 3000 g and the batches were granulated using 1500 g of 15% (w/w) aqueous PVP solution as a binder. The spraying rate was 77 g/min, atomisation pressure was 0.15 MPa and the nozzle height 45 cm from the distributor plate. The inlet air temperature was 40°C during mixing and spraying and 60°C during drying. The inlet air flow rate was adjusted depending on the formulation to obtain optimal fluidisation.

4.3 Powder characterisation

4.3.1 Flowability (I-II)

The flowability of the samples (n=5) was studied using FlowPro instrument (SAY Group, Helsinki, Finland) in controlled conditions (24±1°C, 50±2% RH). The samples were sieved through a 1 mm sieve before the experiments. The funnel of the instrument was cleaned with dry pressurised air prior to each measurement. When samples containing magnesium stearate were measured, the funnel was washed after experiments in order to prevent magnesium stearate from coating the funnel.

The flow rate of the 28 granule batches and three grades of MCC (Avicel PH101, PH102 and PH200) were measured with the photometric 3D imaging method described in the chapter 4.3.2.1. The sample was weighed and fed into a cuvette through a hopper, and the images were taken. The bottom of the cuvette was opened for 0.3 seconds every two

seconds. All samples were measured three times. The flow rate of the samples was calculated by dividing the mass of the sample by the time it took the sample to flow through the instrument.

4.3.2 Particle size (I–III)

4.3.2.1 Photometric 3D imaging (II–III)

In study II, the PSD of 28 granule batches were determined using a photometric 3D surface imaging method (Flashsizer FS3D, Intelligent Pharmaceutics Ltd, Helsinki, Finland). The samples are fed into a chute through a hopper (orifice diameter 40 mm), and the particle size is recorded with 5 s intervals. The number of images and particles measured depends on the shutter opening velocity and the flow rate of the powder. In this case, on average 30 images were taken per batch. The number of particles per image measured varied from 600 to 1600. Approximately 300 g of each granule batch was analysed (n=3). The sampling for the granules was made using a rotary sample divider (Fritsch Sample Divider Laborette 27, Idar-Oberstein, Germany).

In study III, the PSDs of the entire granule batches I-V were measured in triplicate using the procedure described above.

4.3.2.2 Sieving (II)

In study II, the PSD of 28 granule batches were determined by sieve analysis. The granules were sieved using Fritsch analysette sieve shaker and sieves (Fritsch GmbH, Idar-Oberstein, Germany). The sieving time was 5 min with the amplitude of 6. The sieve analyses (range 90–1,400 μm with $\sqrt{2}$ increment) were performed in triplicate.

4.3.2.3 Spatial filtering velocimetry (II)

The spatial filtering velocimetry (SFV) results were obtained using Parsum instrument (Parsum IPP 70; Gesellschaft für Partikel-, Strömungs- und Umweltmesstechnik GmbH, Chemnitz, Germany) as described earlier (Närvänen et al., 2009). The samples (20 g each, n=3) were poured through an orifice (diameter 4 mm) using a funnel and dispersed by pressurized air. The number particle size (chord length) distribution was transformed to volume PSD for data analysis.

4.3.2.4 Laser diffractiometry (I, III)

The particle size of the raw materials in study I and the PSDs of samples (n=3) obtained from batches I-V in study III was determined using Helos laser diffractometer with a Rodos disperser unit and vibrational feeder (Sympatec Gmbh, Clausthal, Germany).

4.3.3 Surface properties (I)

4.3.3.1 Specific surface area

The specific surface area measurements were performed using TriStar 3000 gas adsorption analyser with argon as an adsorbant (Micromeritics, Norcross, USA, n=2). The samples were dried in vacuum at 40°C for 16 hours prior to the measurements. The five-point BET theory (Brunauer et al., 1938) was applied to calculate the specific surface areas of the samples.

4.3.3.2 Carrier payload

Based on the particle sizes of the raw materials, carrier payloads (CP) for the samples were calculated according to Equation 2. CP is the ratio between the total projection surface area of the drug particles and the total outer particle surface area of the carrier particles. A payload below one indicates that the carrier has free surface, while if the CP is more than one, the surface of the carrier is compleely covered with the drug particles (Van Veen et al., 2005).

$$CP = \frac{m_{paracetamol} d_{mean,mcc} \rho_{mcc}}{4 m_{mcc} d_{mean,paracetamol} \rho_{paracetamol}} \quad (2)$$

Where m is the mass of the sample, d_{mean} is the mean particle size of a compound and ρ is the density of a compound.

4.3.3.3 Electrostatic charging

Neutralised samples were charged by sliding powder through a grounded stainless steel pipe into a Faraday cup. The length of the pipe was 500 mm and the inner diameter 25 mm. Prior to the measurements, the pipe was carefully cleaned and placed at the angle of 55° with respect to surface. The method has been explained in detail previously (Murtomaa and Laine, 2000).

4.3.4 Bulk and tap density (I, III)

The bulk and tap densities (d_{bulk}, d_{tap}) of raw m1aterials (study I) and granules (study III) were measured by the European Pharmacopoeia method (Erweka Apparatebau GmbH, Germany, n=3). Carr's index and Hausner ratio were calculated from the bulk and tap densities.

4.3.5 Water activity (I)

The water activity of the raw materials and samples was measured once with AquaLab 3 (Decagon Devices, Pullman, USA). Raw materials were measured prior to and after conditioning and the samples after conditioning.

4.4 Process monitoring (III–V)

4.4.1 Real-time photometric imaging

Each granulation was recorded by a 3D surface imaging device prototype, consisting of a camera connected to an automated sampling double-cuvette attached to the granulator vessel (Flashsizer FS3D, Intelligent Pharmaceutics Ltd, Turku, Finland) (Figure 7). The dimensions of the cuvette were 5*4*1.3 cm and the size of the measurement field was 1.5×1.1 cm. The sampling interval was five seconds and 300 to 450 images were taken per batch depending on the length of the granulation. The number of particles per image measured ranged from 600 to 1700. In the sampling cuvette a pulsed air pressure was used to return the sample to the process between each imaging time-point. The air pulse also cleaned the glass window of the cuvette, preventing window fouling.

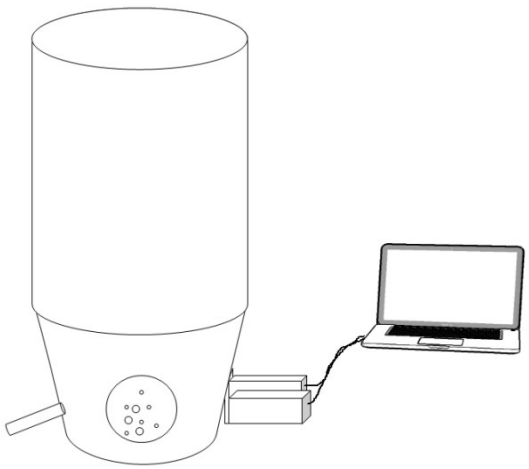

Figure 7. *The set-up for on-line surface imaging and NIR spectroscopy and at-line sampling for fluid bed granulator.*

A variant of photometric stereo (Horn, 1970, Woodham, 1980) at two lights was used to obtain 3D surface of a sample. The samples were presented to the instrument in a continuous feed and imaged through a glass window. The camera was situated horizontally to the window and sample surface. The viewing direction was kept constant, but the direction of the incident illumination was varied. In the method, the light sources were located 180° from each other in a horizontal plane and the angle of illumination was 30°. The resulting gradient fields obtained with the above-mentioned setup contain direct information about surface normal in xz plane and indirect information about surface normal in yz plane. Line integration was used in horizontal direction to obtain a 3D surface. Peaks on the 3D surface are assumed to be particles. The volume (V) based particle size (d) is then calculated from the area of peaks (a) in xy direction:

$$d = \sqrt{a} \times c \qquad (3)$$
$$V = d^3$$

c in Equation 3 is calibration constant, calibrated with six different-sized (100–1400 μm) spherical cellulose particles, cellets (Syntapharm, Mülheim an der Ruhr, Germany).

4.4.2 Real-time NIR spectroscopy

NIR spectra were continuously collected from each granulation process through the double-cuvette sampler with a NIR spectrophotometer over the spectral range 1081–2250 nm (Control Development, South Bend, USA). The range used in the data analysis was 1100 – 2200 mn. The median particle size at each granulation time point was extracted from the untreated NIR spectra by plotting the spectral height (i.e. counts) at 1288 nm against time. The spectral baseline shifts at this wavelength are attributed to particle size changes due to minimal chemical absorption. Moreover, this wavelength has been used for particle sizing earlier (Osborne et al., 1981). The particle size corresponding to each spectral height was obtained by referencing the NIR particle size curves to the image-based particle size curves.

4.4.3 Process measurements

The 1) inlet air flow rate, 2) inlet air humidity, 3) inlet air temperature, 4) outlet air humidity, 5) mass temperature, and 6) outlet air temperature were continuously recorded during processing of the batches. The water amounts of the inlet and outlet air were calculated from the measured relative humidity and air temperature. The total inlet water amount of each process phase was calculated for each batch by multiplying the inlet air water amount by the process time.

4.4.4 Moisture content of samples

LOD of samples obtained at the end of the mixing, spraying and drying phase was measured by IR-drying (Sartorius Thermocontrol MA 100; Sartorius, Göttingen, Germany). The samples were measured in 105°C and the sample weight was 3–5 g.

4.5 Data analysis

4.5.1 Partial least squares (I)

A PLS model using cross-validation was created using the Simca-P software v 10.1. (Umetrics AB, Umeå, Sweden) to evaluate how well the physical factors measured predicted the measured powder flow behaviour. The predictive abilities of the models were described using R^2 (goodness of fit) and Q^2 (goodness of prediction) values on a scale from 0 to 1.

4.5.2 Apparent water absorption (IV–V)

Moisture content was determined from the NIR data using the baseline corrected and normalised apparent water absorption (AWA) values. The calculation of AWA is shown in equation 4 and has been described earlier (Rantanen et al., 2000).

$$\text{AWA} = \frac{-\log 10\left(\frac{\text{Ix}}{\text{Ix,ref}}\right)+\log 10\left(\frac{\text{Iy}}{\text{Iy,ref}}\right)}{\log 10\left(\frac{\text{Iz}}{\text{Iz,ref}}\right)+\log 10\left(\frac{\text{Iy}}{\text{Iy,ref}}\right)} \quad (4)$$

where I is intensity (x referring to 1998 nm signal, y to 1813 nm signal, and z to 2214 nm) and ref is intensity using aluminum plate reference at the corresponding wavelength channel.

4.5.3 Analysis and visualisation of NIR data (IV–V)

Matlab software (MathWorks, Natick, USA) was used for analysing and visualising the NIR data.

In the end of each process, NIR spectrum contains information only on the absorbance or diffraction caused by particle size since all water has been removed. Thus, the final spectrum reveals the shape of the particle size spectrum of the dry material, which is the same at every wavelength. This shape was subtracted from each individual spectrum in

order to remove the influence of particle size and reveal the impact of water on the spectra. The variance in the amount of absorption that arises from particle size was compensated by scaling the shape values to match the spectral intensity. This procedure was needed if the particle size was different from the final granule particle size. The scaling value at each time point was obtained from particle size determined earlier (1288 nm).

5 Results and discussion

5.1 Flowability (I–II)

5.1.1 Powder flow

The flowability of the binary mixtures of MCC and paracetamol decreased when the amount of paracetamol increased, which results from the platelike morphology and small particle size of paracetamol. The decrease in flowability was the most notable at low drug loading. Additional increase in drug loading above 12.5% did not affect the flowability as significantly as at lower concentrations. However, as expected, the flow rate depended also on the MCC grade: the samples containing Avicel® PH200 and PH102 had the best and the mixtures of PH101 and paracetamol the poorest flowability. Magnesium stearate was able to increase the flowability of PH102 and PH200 samples but not the ones containing PH101 (Figure 8).

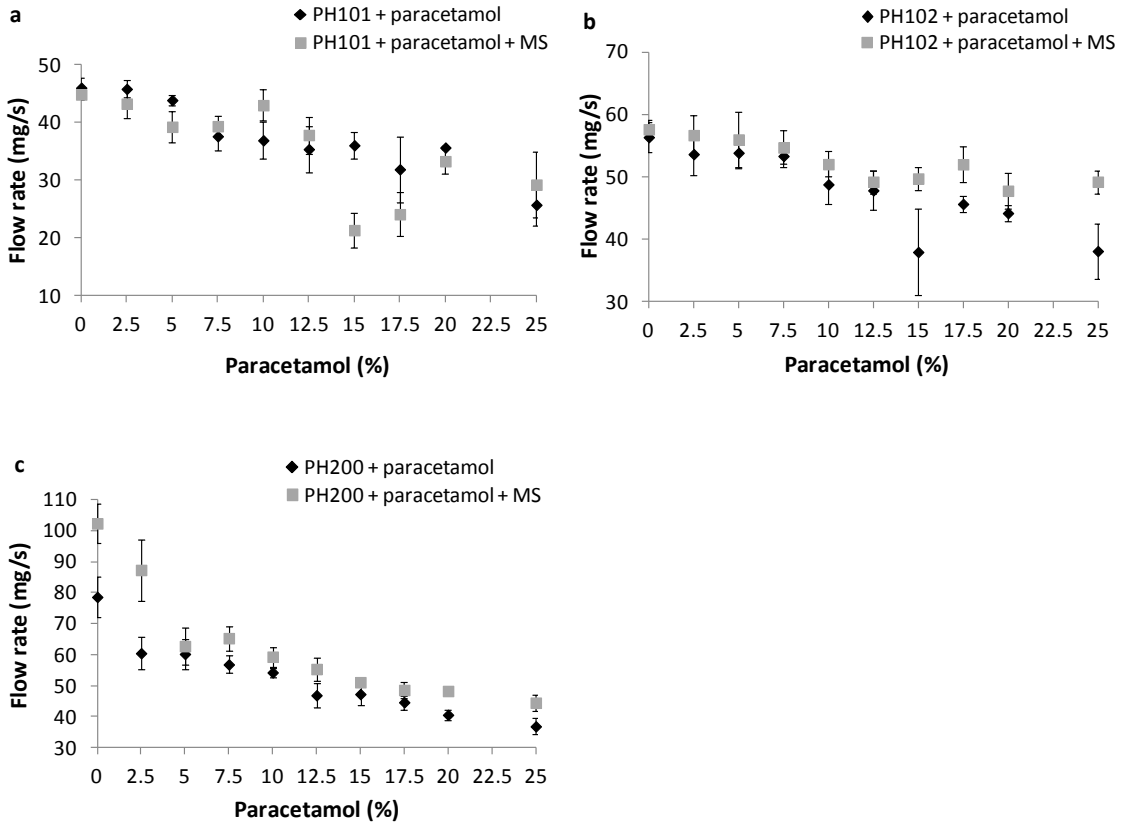

Figure 8. *The effect of paracetamol concentration and magnesium stearate (MS) on the flow rate of binary mixtures of paracetamol and a) Avicel® PH101, b) PH102 and c) PH200.*

The PLS model revealed that carrier payload and particle size are the most important factors influencing the flowability of the binary powder mixtures (Figure 9). Nevertheless, all other physical properties measured had an impact on the flow behaviour. In general, the powder flow measurements performed provided information on the behaviour and similarity of materials.

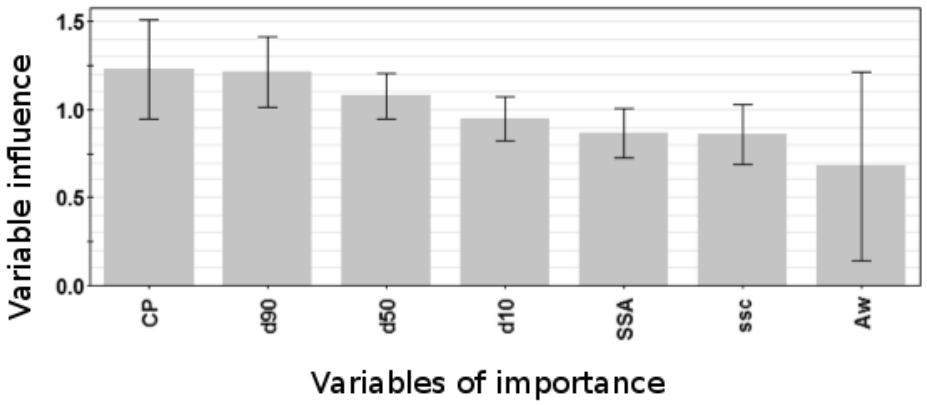

Figure 9. *Variables of importance (VIP) plot of the PLS model for prediction of powder flow. CP carrier payload, d_{90}, d_{50}, d_{10} = descriptors for particle size distribution, SSA = specific surface area, ssc = spesific surface charge, A_w = water activity. Terms with larger VIP than 1 are the most relevant for explaining flow.*

The phenomena affecting powder flow of the binary mixtures are complex and thus several aspects such as tribocharging, carrier payload and surface moisture need to be taken into account when assessing powder flow behaviour and choosing suitable excipients for formulations.

If the relationships between these flow measurements and e.g. mass variation during tableting or capsule filling can be established, the methods could provide a fast small scale screening tool for choosing direct compression excipients and optimal drug loading levels to be used in formulations. Modelling the impact of the key powder properties on the flowability could enable the optimisation of the formulation parameters to reach the target flow rate.

5.1.2 Granule flow

The flow rate of the granules obtained during photometric PSD measurement ranged from 1.6 to 5.9 g/s. The weight variation of tablets decreased with improved granule batch flowability until a critical median granule size was reached (Figure 10). Larger median granule size has been shown to increase tablet weight variation (Laitinen et al., 2004).

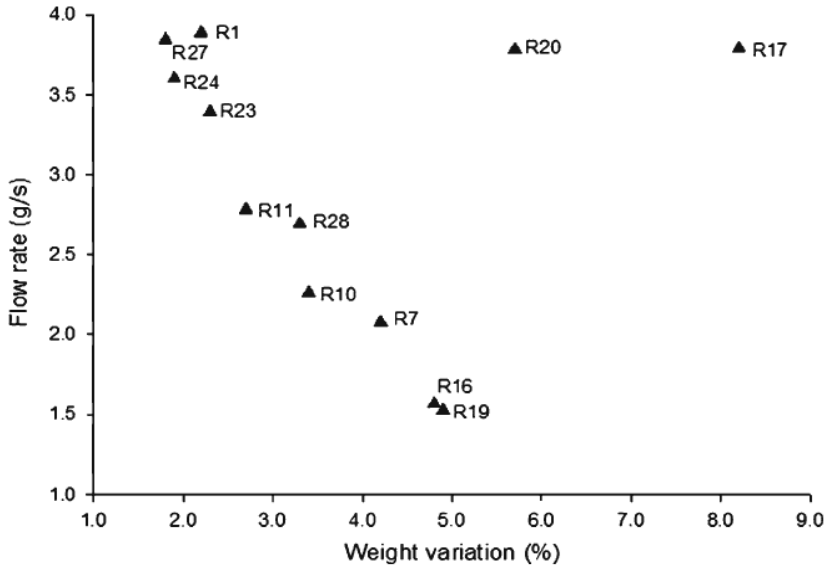

Figure 10. *Impact of the flow rate of 12 granule batches on the weight variation of corresponding tablets. Above a critical granule median size, flowability does not correlate to weight variation (R20 and R17).*

5.2 Granule size distribution (I–II)

The applicability of 3D photometric imaging on measuring PSD of entire granule batches was studied (II, III). The results were compared to sieve analysis and SFV (II) (Figure 11) and laser diffractometer (III). The Pearson's correlation values for the d_{10}, d_{50} and d_{90} values were: image vs. sieving (0.55, 0.82, 0.84), image vs. SFV (0.95, 0.82, 0.34) and SFV vs. sieving (0.72, 0.64, 0.35). Generally, the best correlation is between the d_{10} and d_{50} values of SFV and image. Sieving in general indicates a shift towards the smaller size compared to the other techniques due to the friability of the brittle granules. By contrast, the larger d_{90} values measured by SFV in comparison to the other techniques are likely to arise from SFV interpreting two middle-sized particles as one large granule.

By contrast to SFV, photometric imaging is often able to recognise agglomerates as different particles. Also, the measured chord length distribution in SFV depends on the orientation and location of a granule, which results in a broader PSD (Närvänen et al., 2009).

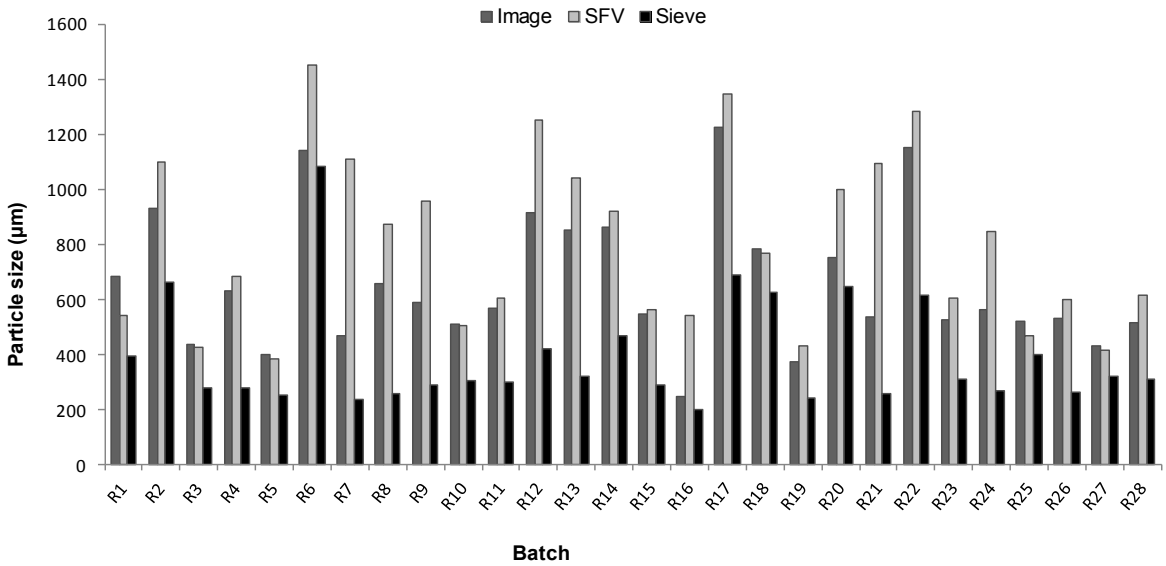

Figure 11. *The d_{50} particle size values of 28 granule batches measured by photometric imaging, SFV and sieve analysis.*

Compared to laser diffractometer, photometric imaging generally suggests larger particle sizes for granules containing MCC. However, the d_{50} values of lactose granules obtained from images and laser diffraction are rather similar, 881 µm and 827 µm, respectively. The deviation between the methods generally grows with increasing MCC proportion and presumably originates from the breakage of the fragile MCC-containing granules during handling, sampling and laser measurements. Vibratory impact can reduce particle size and high laser diffractometer dispersion pressure leads to size reduction of fragile granules (Antonyuk et al., 2006, Silva et al., 2013).

Some of the deviation between the different methods arises from their different measuring principles and the fact that they generally assume the particles to be smooth and spherical (Andres et al., 1996, Shekunov et al., 2007). Thus, a considerable strength of surface imaging compared to laser diffraction is that the reliability of the results can easily be evaluated from the images. Another advantage of the photometric method is that the samples are presented to the instrument in a continuous feed and a large amount of granules can be analysed without sampling. Moreover, the analysed sample can be used for other purposes after the analysis due to the non-destructive nature of the imaging procedure. The sieving process wears down granules and can cause tribocharging of especially small granules leading to errors in the particle size results. On the other hand, shades inside an irregular particle may lead to the imaging instrument interpreting the particle as more than one. The misinterpretation could potentially be reduced with improved instrument resolution or lightning.

Moreover, the 3D figures demonstrate the usefulness of image information in powder and granule characterisation. The figures do not only show the particle size of the granules but also the morphology and surface texture. They also give an idea on the PSD and packing behaviour of the granules (Figure 12).

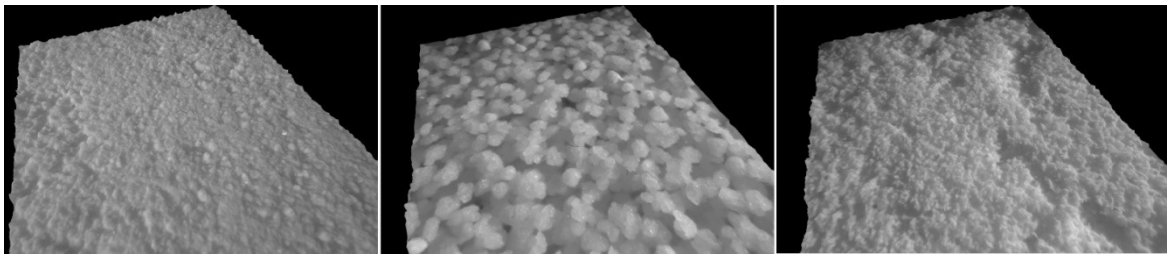

Figure 12. *Three dimensional images provide information on particle size distribution, surface texture and granule packing.*

5.3 Monitoring granule formation by photometric imaging (III)

During fluid bed granulation, lactose forms granules rapidly and majority of the growth occurs during the first 2–3 minutes of spraying (Figure 13). However, introduction of MCC into the formulation slows down the granule growth rate leading to a rather constant growth throughout the spraying phase. When granulation liquid has been sprayed for one minute, agglomeration of lactose has begun but the majority of the formulation is powdery. The MCC batch remains very powdery after one minute of spraying. After three minutes of spraying, MCC has formed a fluffy yet powdery mass while lactose is mainly granular. At the end of the spraying phase, MCC has formed very weak agglomerates. The granulation behaviour of all binary formulations is relatively similar but the particle size reducing effect of increasing amounts of MCC can be seen in the images. The granule growth reducing effect of MCC is particularly clearly visible in the images captured from batch II: relatively decent granules are formed but the growth is slow.

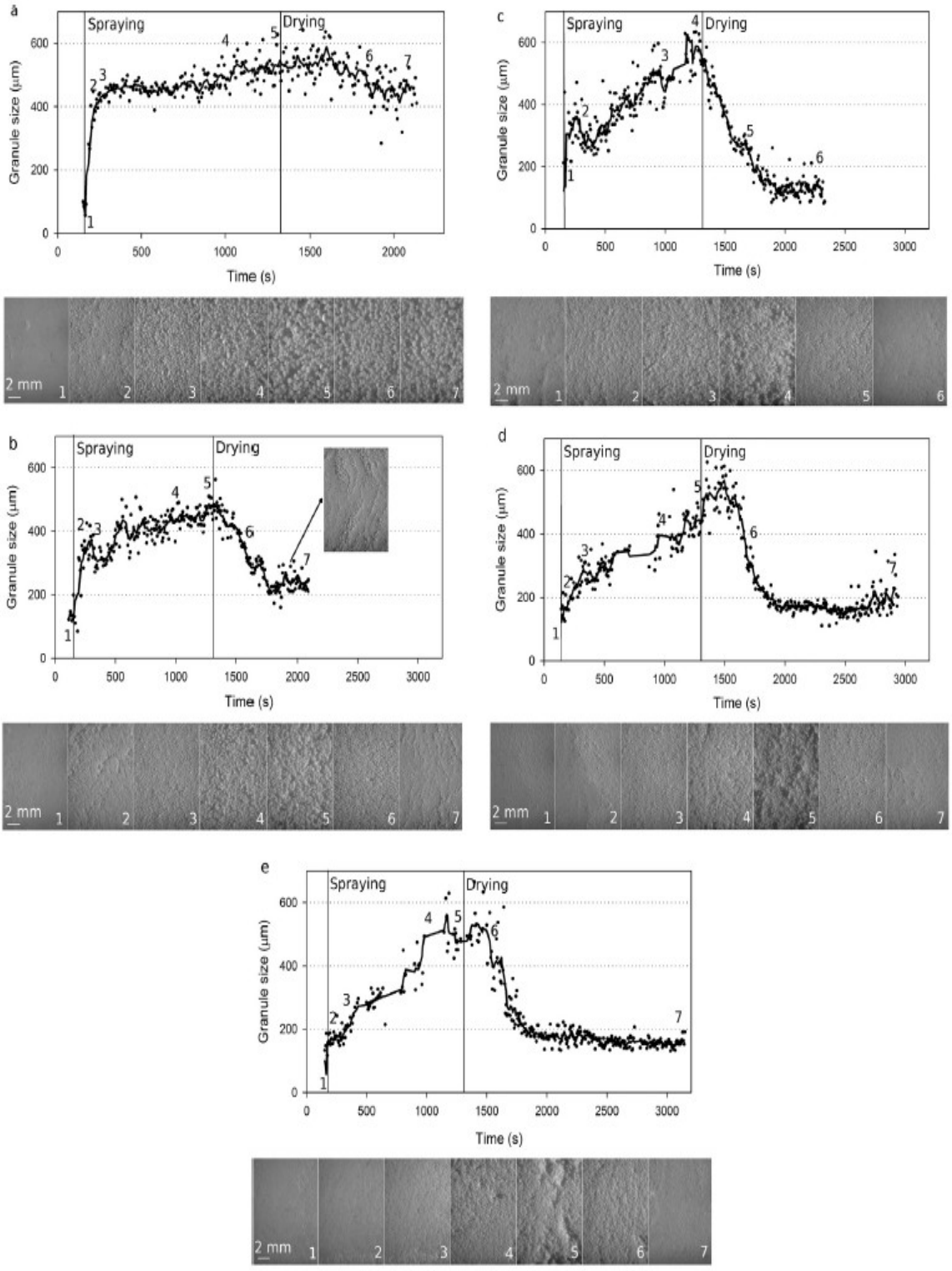

Figure 13. *Granule formation and particle size during fluid bed granulation evaluated by photometric imaging of batches I–V (a-e, respectively).*

In the drying stage, the lactose granules retain their particle size with only slight diminution in the end (Figure 13a). By contrast, batches containing MCC are characterised by a rapid size reduction, which accelerates with increasing MCC amount, after the granulation liquid feed is stopped (Figure 13b–e). The final granule size of batches containing MCC ranges from 180 to 200 µm compared to 470 µm for lactose. The final particle size in batches that contain at least 50% MCC is also very close to that of the initial powder. Attrition of formulations containing a large amount of MCC compared to lactose has been earlier explained to result from the longer drying time of MCC (Rantanen et al., 2001a). However, the current surface imaging approach revealed that the MCC granule breakage takes place immediately when drying is started. The particle size of batches IV and V decreases rapidly during drying until almost the initial starting material particle size is reached (Figure 13d–e). Approximately at the same time, the mass temperature begins to increase faster (Figure 14a) and the outlet humidity begins to decrease after the initial increase (Figure 14b). Thus, fast breakage of the granules appears to occur as long as water is rapidly removed from the mass. Fines have been reported to form when the bulk water content is below 6% (Bika et al., 2005). Further drying also accelerates the formation of fines. By contrast, at water contents higher than 6% fines formation is negligible.

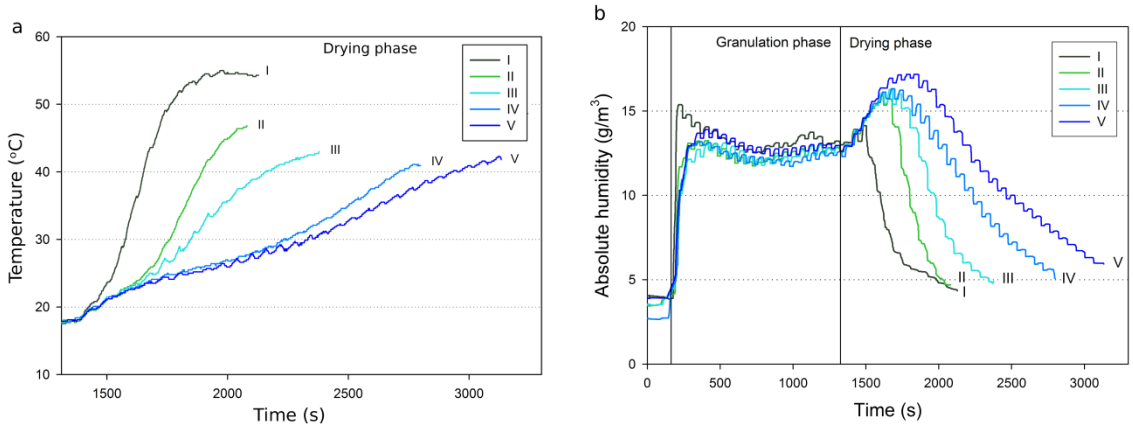

Figure 14. *Granule bed temperatures of batches I–V during the drying phase (a) and absolute outlet humidity of the granulator during granulation (b).*

Compared to the photometric method, NIR spectroscopy suggests smaller particle sizes in the spraying phase and faster size reduction of batch I during drying (Figure 15). The attrition behaviour of the other formulations was similar in both methods. At the end of the spraying phase, the median granule size in batch I measured by NIR spectroscopy and images was very similar. However, images suggest larger particle sizes for the other batches and the difference between the methods grows with increasing MCC proportion. The final particle sizes of batches I–III measured by NIR correlate well with the image data but the images gave again larger results for the batches IV and V. Based on these findings, the surface imaging method can efficiently calculate the particle size of dense and well-packing granules. However, the accuracy of the particle size measurements

decreases when poorly-packing powders are measured. Yet, the particle size trends can be followed by the imaging method throughout the granulation process.

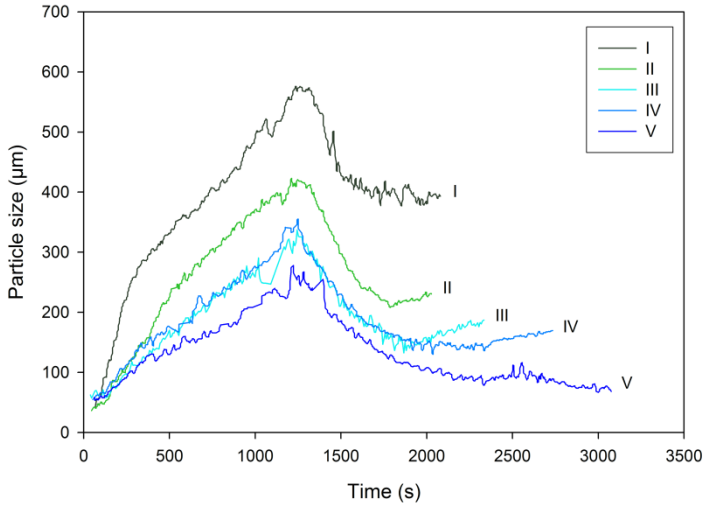

Figure 15. *The median particle size of each granule batch measured by on-line NIR spectroscopy at the wavelength 1288 nm.*

The current results suggest that already a minor amount of MCC absorbs the granulation liquid so rapidly that adequate liquid bridge formation between the colliding particles is hindered. Thus, the liquid bridges are broken during drying before the particles can form solid bridges. Moreover, in formulations containing water soluble filler and binder, the solid bridges are formed by coprecipitation of the filler and polymer (Bika et al., 2005). Thus, the disparity between lactose and MCC in the drying step is likely to arise partly from lactose and PVP coprecipitating to form strong solid bridges unlike the non-water soluble MCC. The ability of binders to bind different fillers also varies (Bika et al., 2005).

It has been proposed that granule growth behaviour can be divided into two groups: steady and induction growth (Iveson and Litster, 1998). Steady growth is typical for deformable and weak granules that have a large contact area. By contrast, slowly consolidating granules are not able to form a strong bond due to insufficient deformation. Thus, the collided granules break apart rapidly leading to an induction period with little or no granule growth. In the light of this theory, rapid growth appears to be typical for lactose and induction growth for MCC.

5.4 Continuous moisture measurements (IV)

This chapter describes and discusses the use of AWA and water balance as continuous moisture analysis methods during fluid bed granulation. The chapter is divided to 1) lactose, 2) MCC and 3) their mixtures to highlight the characteristic behaviour of the

different materials. General remarks on the different measurement techniques are discussed at the end of this chapter.

5.4.1 Lactose

The water contents of the batch 1 samples are generally very close to water balance, except for the sample taken five minutes before stopping the process (Figure 16). Moreover, the AWA and water balance of batch 1 are generally rather similar (Figure 17a). The saw tooth structure of the AWA curve results from granule drying and thus the higher edge of the curve describes the moisture content. The overall similarity between the methods indicates that practically all added water is rapidly removed from the lactose granules during the measurements. The rapid dehydration of lactose surfaces upon drying is likely to explain this (Ticehurst et al., 1996). The rapid drying arises from water filling the empty spaces in lactose instead of being strongly bound (Clydesdale et al., 1997).

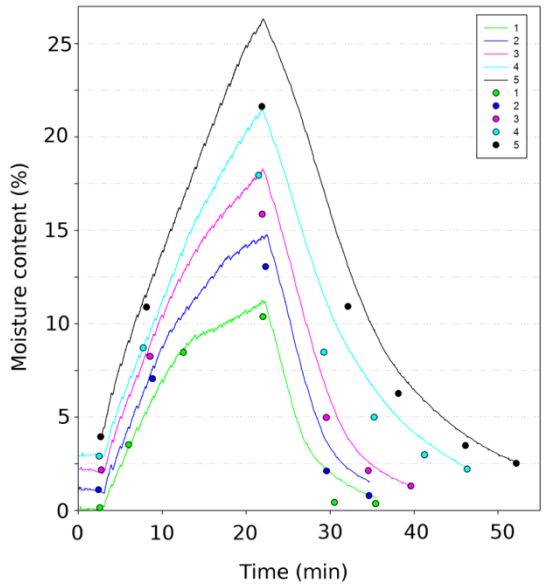

Figure 16. *Water balance (solid lines) and sample moisture content (circles) measured by infrared drying in batches 1–5 during granulation.*

During the last minutes of the process, the AWA and LOD values are similar but slightly lower than the water balance (Figure 16, 17a). The proximity of the sample moisture contents collected at the end of the process and five minutes before the end indicates that granule drying was complete already a few minutes before the end. The batch also reached a constant bed temperature, which is an indicator of completed drying, at the same time-point in an earlier study (Figure 14a). Both the AWA and LOD measure water content directly from the granules whereas the water balance is the amount of water in the process. The higher water balance values suggest that water has been removed from the granules but not yet from the granulator. The residual water could thus be in the process air or condensed in the filter bags.

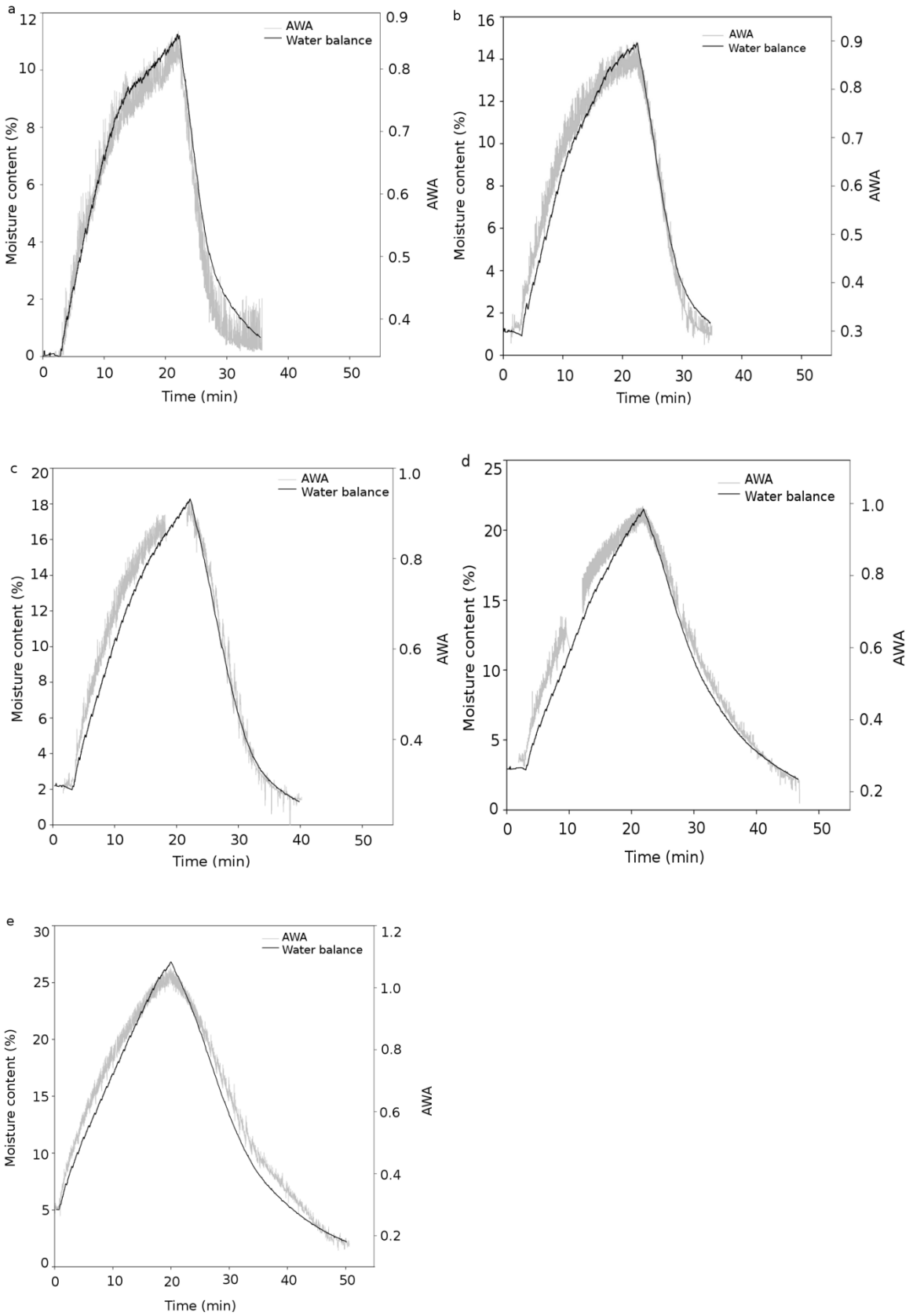

Figure 17. *Water balance and apparent water absorption (AWA) of batches 1–5 (a–e, respectively).*

The slopes of the water balance and AWA curves in batch 1 decrease notably after approximately 10 minutes of liquid spraying (Figures 16 and 17a). A similar phenomenon is visible in the NIR moisture content measured during the granulation of batch consisting principally of lactose (Otsuka et al., 2014). The observed transition is likely to result from the wetting saturation of lactose being reached, which could lead to lactose surfaces dissolving in the adsorbed water (Kontny and Zografi, 1995, Schaafsma et al., 1998). An increased outlet air humidity, which indicates decreased moisture sorption by the formulation, at the same time point (Figure 14b). Moreover, the water balance transition at the end of the drying phase (at around 30 min) occurs at the same time with the bed temperature reaching a plateau.

5.4.2 MCC

In the batch 5, the LOD values are generally lower compared to water balance (Figure 16). The difference is the most pronounced in the end of the spraying phase, approximately 5%, which is close to the amount of bulk water in MCC. Since the correlation between LOD and water balance is generally better in the early spraying phase, processing appears to change the structure of MCC in a manner that contributes to water retention in the matrix. The conclusion is supported by practically complete water removal unprocessed MCC wetted with PVP solution (Table 4). Moreover, up to 6–8% water in MCC can be unavailable (Zografi et al., 1984). Added bulk water is not physically bound to MCC but wet granulation and drying alters the C-H bonding in MCC (Fielden et al., 1988, Zografi and Kontny, 1986, Buckton et al., 1999). Thus, some residual moisture could get trapped in MCC by diffusional barriers (Zografi and Kontny, 1986).

Table 4. *The measured and theoretical moisture contents of samples consisting of bulk MCC powder and 15% PVP solution in different temperatures (n=3).*

Measuring temperature (°C)	Bulk MCC moisture content (%)	Measured moisture content MCC + PVP (%)	Calculated moisture content MCC + PVP (%)	Difference, calculated / measured (%)
105	3.9	28.5	29.4	0.9
135	4.0	28.9	29.9	1.0
150	4.1	24.3	25.4	1.1

The proximity of water balance and AWA at the end of the process indicates that all free water has been removed from the granules as well as the granulator. Moreover, a change in drying kinetics of the batch 5 is visible in the water balance and AWA curves around 36 minutes of granulation. A simultaneous increase in the granule bed temperature occurs (Figure 14a). The change results from the transition from the initial water diffusion through the solid phase to water vapor diffusing through the material pores (Wildfong et al., 2002).

5.4.3 Mixtures of lactose and MCC

The maximum water balance values at the end of the spraying phase in batches 2, 3 and 4 are 15, 18 and 22 %, respectively (Figure 17). The corresponding LOD results are 2–3% smaller and the deviation grows with increasing moisture content and MCC proportion. The rather steady increase in the moisture content of the wettest samples with increasing MCC proportion suggests that the ability of the formulation to take up water depends linearly on the amount of MCC. This results from the ability of MCC to absorb a large amount of water by contrast to lactose (Ek and Newton, 1998, Schaafsma et al., 1998).

A transition in the water balance and AWA curves in the late spraying phase resulting from wetting saturation of lactose surfaces is clearly visible also in the batch 2 and slightly visible in the batch 3 (Figure 17b–c). However, it is practically absent in batch 4. Moreover, the drying kinetics and time in the batches 2–3 resemble batch 1 while the drying behaviour of batch 4 is closer to that of batch 5. Furthermore, the change in the drying kinetics and times is larger between batches 3 and 4 compared to other batch-to-batch differences. Thus, the moisture sorption and retention capacity is clearly a critical point when the proportion of MCC increases from 50% to 75%. Furthermore, the transitions in the water balance slopes during drying of batches 2–4 appear at the same time points as the bed temperature changes (Figure 14a).

In general, the maximum water balance values as well as the curve kinetics reflect the water sorption capacity of the formulation. MCC can take up large amounts of water, which is reflected in higher water balance levels compared to lactose. While the amount of water adsorbed to crystalline materials depends on the available surface area, amorphous materials can absorb water proportional to their mass (Ahlneck and Zografi, 1990). In the current study, the non-saturating water balance curves suggest that the maximum water uptake capacity of MCC is not reached during the process. The water balance curves also reveal the differences in the moisture loss tendency of the different batches. Lactose has a steeper slope in the drying phase compared to MCC. The drying time of MCC is also much longer and results in higher final moisture contents with formulations containing a larger proportion of lactose.

5.4.4 Remarks on the different techniques

The differences between the off-line, water balance and AWA moisture measurements are partly attributed to the water they measure. AWA and the LOD methods measure the water content of the sample while water balance does not specify the location of water in the granulator. AWA appears to be the most reliable method for accurate determination of the total water content of the mass while the LOD methods seem to be limited to measuring only unbound water. The accuracy and precision of AWA are enabled by collecting data at very frequent intervals from static sample through a self-cleaning window. Considering that the in-line water balance measures the water amount in the whole process, it generally gives a good estimate on the mass moisture content. The connection between changes in water balance and bed temperature confirms that water balance is a suitable tool for monitoring the moisture sorption and loss behaviour of

different formulations. Combined with AWA, water balance can reveal the water proportion in the mass compared to other locations in the granulator.

5.5 Image brightness and granule drying (III–IV)

Increase in pellet surface brightness has been shown to correlate with drying (Burggraeve et al., 2011a). However, the surface brightness of granules decreased during drying (Figure 18). Moreover, the image brightness of batches IV and V remained unchanged for approximately 250 seconds in the middle of drying, simultaneously with the transition in mass temperature kinetics (Figure 14a). Plateaus in the brightness curves occurred simultaneously with transitions in bed temperature, AWA and water balance. The results suggest that decreasing granule surface brightness is an indicator of drying for lactose monohydrate and MCC granules. This results from reduced granule surface reflectivity at lower water amounts. Image brightness has previously been shown to increase as long as water was removed from pellets and theophylline monohydrate was converted into the anhydrous form (Burggraeve et al., 2011a). Comparison between the earlier and current results shows that change in the image brightness is connected to granule or pellet drying. However, the direction of the change depends on the formulation, dosage form, the location of water in the product and the occurrence of polymorphic changes. The impact of these individual properties is not fully understood yet and is subject to further studies.

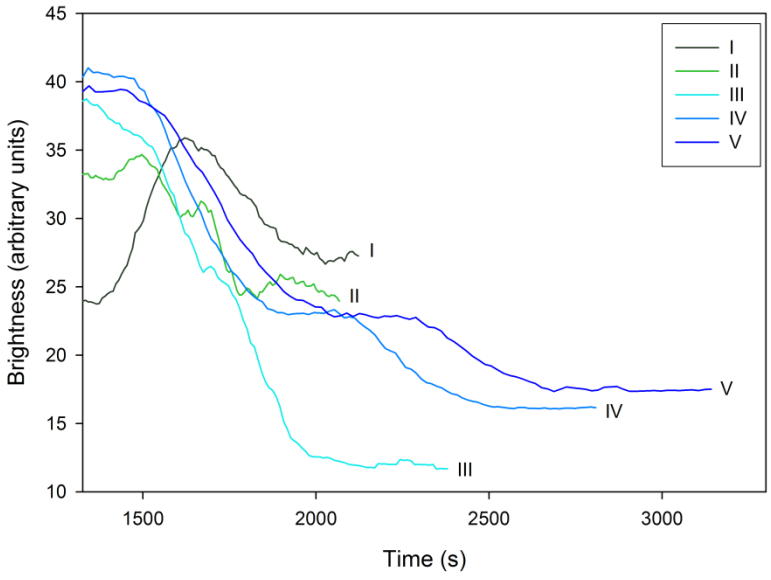

Figure 18. *Image brightness during drying of different granule formulations.*

In addition to the correlation with bed temperature and outlet humidity, the transitions in image brightness curves appear at the same time with the transitions in the water balance and AWA slopes during drying of batches 2–4 (Figures 16–17). Moreover, a change in drying kinetics of the batch 5 is visible in the water balance and AWA curves around 36

minutes of granulation, simultaneously with an image brightness plateau and increase in the granule bed temperature and, which both indicate granule drying.

5.6 Monitoring changes in particle size and moisture content during fluid bed granulation (V)

5.6.1 Overview of the spectral treatment

An example of the spectra divided with the starting material spectrum is shown in Figure 19. The first divided spectrum is a straight line with a value of one (Figure 19b). The treated spectra contain information only on the changes occurring during granulation. Thus, the observed changes such as peaks and baseline shifts arise primarily from changing particle size and water amount. The granule growth is seen as spectral baseline shift when the granulation liquid amount increases. Moreover, the water peaks at both 1450 and 1930 nm grow as a function of added water, which is effectively visualised by the spectral treatment. The linear increment of 300 g water is not seen between the last two spectra in Figure 19b is also smaller compared to the previous spectra. This suggests that the water absorption capacity of the formulation is close to saturating.

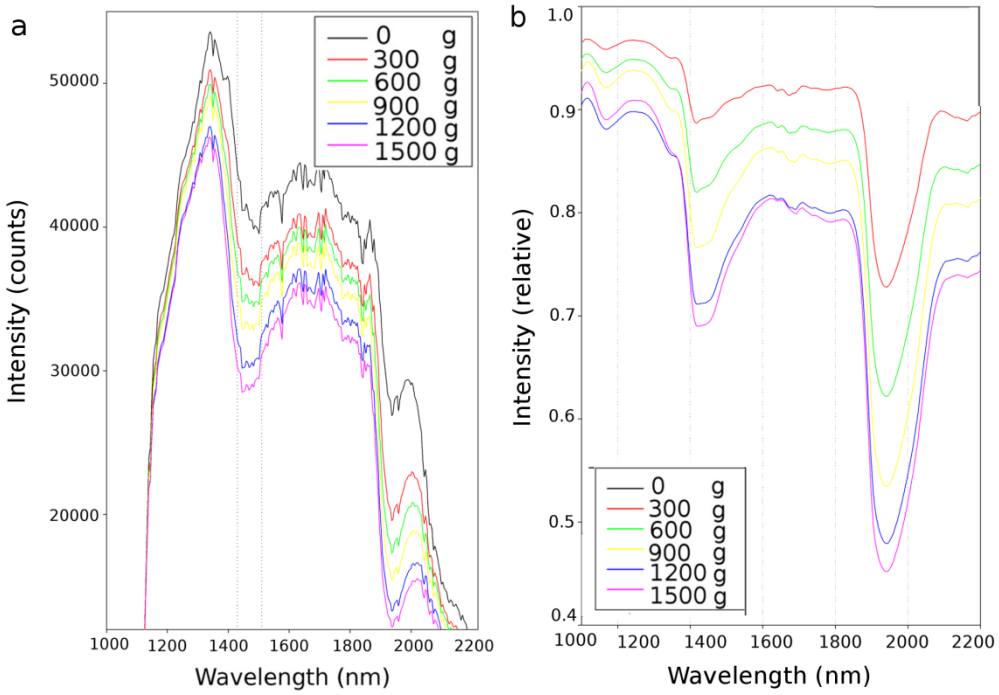

Figure 19. *Examples of the raw (a) and treated (b) NIR spectra of MCC collected from a fluid bed granulation process.*

5.6.2 Lactose

Increased NIR absorbance is observed in the treated data collected from the batch 1 especially around the water peak areas of 1450 nm and 1930 nm (Figure 20a). A rapid upward baseline shift occurs during the spraying phase at wavelengths above 1400 nm. The shift is caused by particle size growth and is more significant at higher wavelengths (Alcala et al., 2010, Gupta et al., 2004). Moreover, the water peaks diminish rapidly during drying but only small return in the baseline occurs, which indicates rapid water removal and little change in particle size. Alcala and colleagues (2010) reported a slight return in the spectral baseline during the drying phase, which correlated to the observed attrition. In the current study, the moisture content and particle size separated from the treated spectra confirm that particle size growth accounts for the baseline shift (Figure 19b–c). The spectral baseline remains unchanged in the image representing moisture content while significant displacement of the baseline dominates the particle size figure. The uneven structure of lactose at 1540–1800 nm is related to the orientation of crystal lattices (Figure 20a) (Nieuwmeyer et al., 2007a).

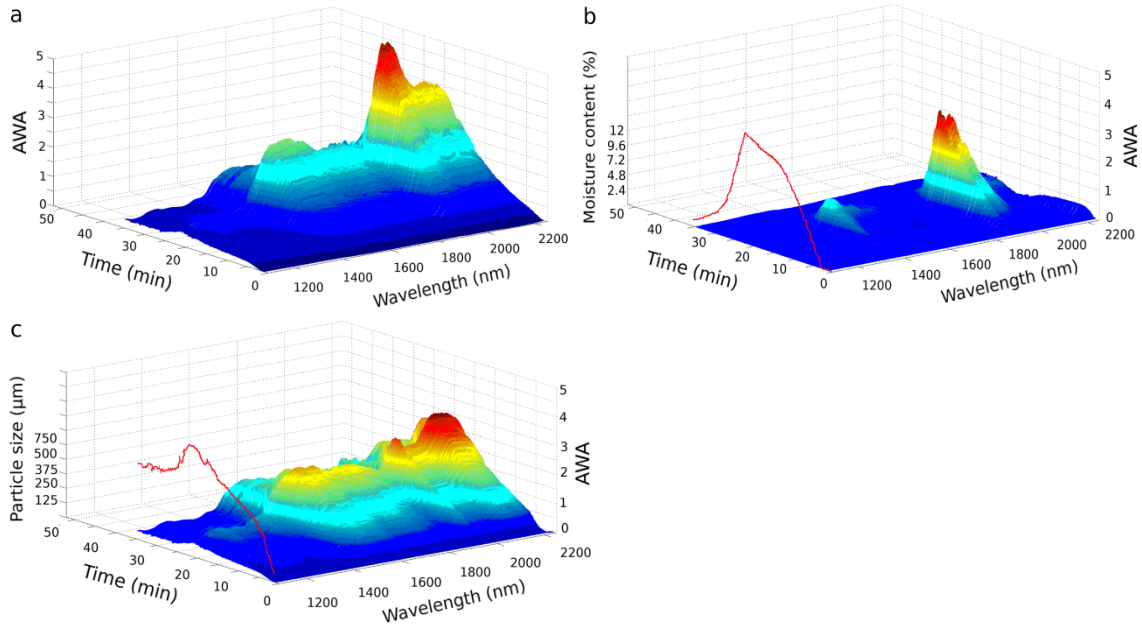

Figure 20. *NIR spectra of lactose during granulation a) the treated spectra; b) the contribution of moisture to the spectra; c) the contribution of particle size to the spectra.*

The addition of granulation liquid as well as the rapid drying of lactose is also clearly visible as growing water peaks and a subsequent rapid decrease in the water peaks in the batch 1 (Figure 20b). The shape of the 3D water peak around 1930 nm generally matches the AWA curve. However, the 3D water peak is unable to reveal the change in surface adsorption rate of water that is clearly visible in the AWA curve (Figure 20b). The water peak around 1450 nm is very small compared to 1930 nm water peak. Higher wavelengths generally indicate greater hydrogen bonding and free water (Martin, 1993).

The particle size changes are seen as notable overall shift in the spectral baseline during processing as well as increased tilt between the lower and higher wavelengths (Figure 20c). The particle size decreases rapidly in the beginning of the drying phase and then remains constant. The particle size plotted using absorbance at 1288 nm is comparable to the shape of the 3D particle size curve as a function of time (Figure 20c).

5.6.3 MCC

The treated spectra of batch 5 are characterised by very small baseline increase and relatively large water peaks, particularly around 1930 nm (Figure 21a). However, the water peak at 1450 nm can be distinguished from the baseline more clearly than in the other batches. This is logical as the 1450 nm indicates a less free state of water than the longer wavelength (Burns and Ciurczak, 2007). The process spectra and the moisture content spectra are almost identical (Figure 21a–b). Majority of the changes in the spectra are connected to water amount since the particle size changes are negligible (Figure 21b–c). Moreover, the shape and height of the AWA curve also equals the 3D water peak.

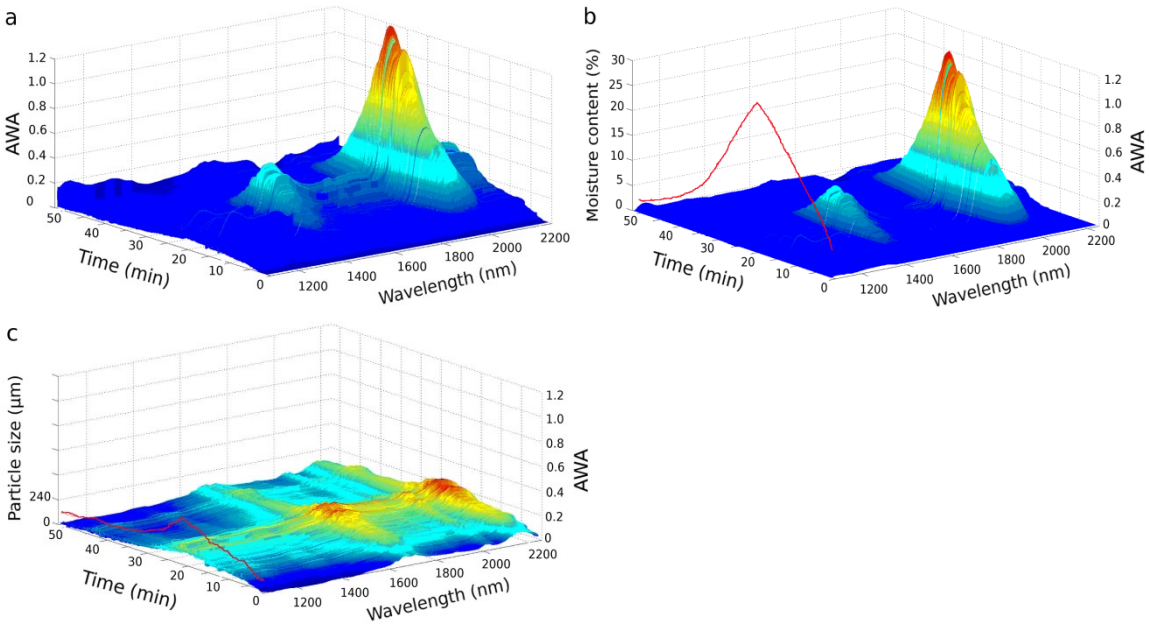

Figure 21. *NIR spectra of MCC during granulation a) the treated spectra; b) the contribution of moisture to the spectra; c) the contribution of particle size to the spectra.*

The influence of particle size on the spectra in the MCC batch is negligible and the baseline returns quickly to the starting level during drying (Figure 21c). However, the spectral region 1610–1900 nm remains practically unchanged in MCC after drying for 12 minutes and until the end. The spectral intensity and shape also differ from the starting

material at this region reveling that a change in the material properties has occurred during processing. Because the peaks between 1540 and 1900 nm often indicate crystal orientation (Nieuwmeyer et al., 2007a), the results could arise from permanently changed particle orientation or increase in the crystalline content of MCC. Also the images captured from the process show that only minor changes in particle size occur during the process (Figure 13e).

5.6.4 Mixture of lactose and MCC

The process spectra of batch 3 is characterised by moderate baseline shift and a large water peak at 1930 nm (Figure 22a). The smaller water peak at 1450 nm is visible but merges into the increased baseline above 1500 nm. Again, the absence of baseline shift in the water content figure, visible in the particle size figure, confirms that the baseline shift results from particle size (Figure 22b–c). The moisture content was separated successfully and the smaller water peak is more defined in the separated moisture content image (Figure 22b). Both water peaks grow rather steadily as a function of time during the spraying phase. A slightly faster drying compared to wetting is also apparent from the spectra. The AWA curve is very similar to the shape and height of the water peaks. The moisture content decrease rapidly when drying is started.

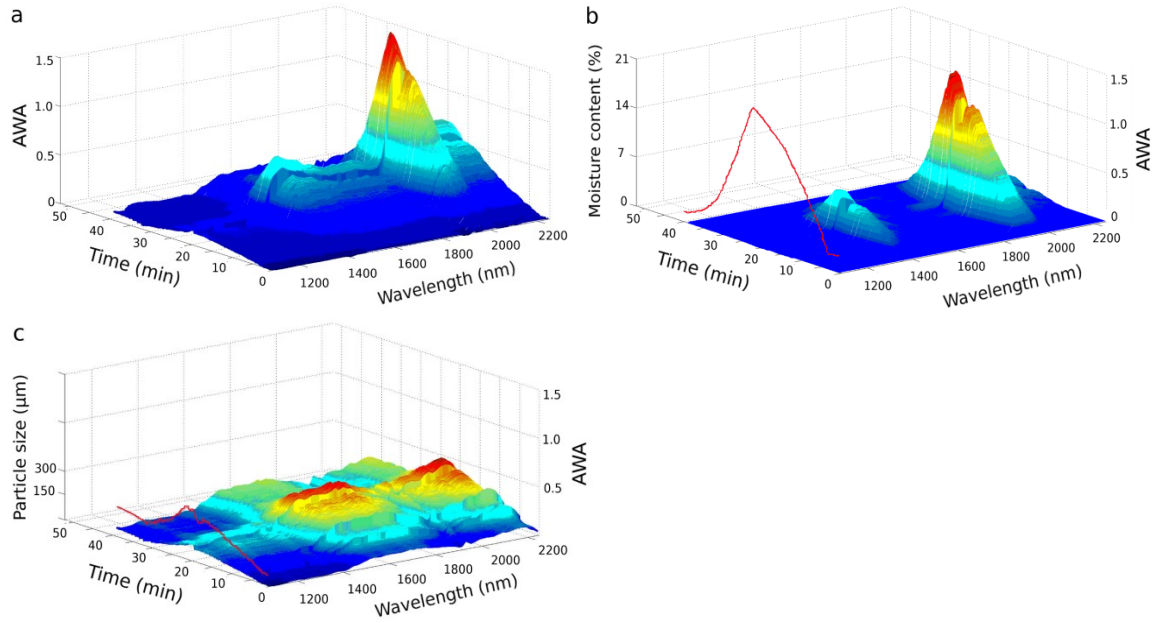

Figure 22. *NIR spectra of a granule batch containing lactose and MCC (50 % each) a) the treated spectra; b) the contribution of moisture to the spectra; c) the contribution of particle size to the spectra.*

The spectral baseline begins to shift when liquid addition is started (Figure 22c). Particle size influences the spectra especially at wavelengths 1400–1900 nm and above 2000 nm.

A notable decrease in the spectral baseline occurs immediately when drying is started, which results from rapid granule attrition. The phenomenon has been captured by surface imaging (Figure 13c).

5.7 Complementary process analytical tools (III–V)

The current results demonstrate that images from the entire granulation process provide valuable information on material characteristics and performance during manufacturing. In addition to PSD, the images revealed batch specific granule growth and attrition behaviour in real time. The changes in granule size were clearly linked to the continuously measured process moisture and temperature conditions. The continuous moisture measurements based on process air moisture content and NIR spectroscopy provided real-time information on the moisture content as well as the batch moisture profile during processing. The comparison of the methods also enabled the evaluation of the location of water in the process. Thus, research and development could benefit enormously from increased use of visual information coupled with complementary process analytical tools. For example, images could give valuable insight into the behaviour of new excipients or formulations during processing. Another great advantage of modern process analytical methods is the creation of extensive data library. It enables systematic data analysis for further process improvements, design space creation and facilitated scale-up. The significance of collecting and recording complementary process data in a continuous fashion will become even more pronounced in the future when the manufacturing processes become automated to a larger extent.

6 Conclusions

A novel small scale flow measurement device proved to be suitable for rapid flowability screening of different formulations. Specifically, the impact of physical properties of the formulation, such as drug loading, on the flowability could be distinguished. The decrease in flowability was the most notable at relatively low drug loadings. Additional increases in drug concentration above 12.5% had only a minor impact on the flow rate.

Photometric imaging was shown to be suitable for measuring the PSD of entire granule batches using a specially designed feeding system. The instrument has the potential for rapid flowability screening and the flowability information obtained in the study also correlated well with the weight variation of tablets compressed from the studied granules. The method was also suitable for continuous monitoring of particle size changes of dense granules during granulation. However, its accuracy is compromised if decent granules are not formed. The images provided direct real-time information on the growth, attrition and packing behaviour of the batches. Moreover, decreasing image brightness during drying reflected the removal of water from the granules. The unrivalled feature of photometric imaging is that the continuously captured images provide direct visual information coupled with numerical data.

The in-line water balance and on-line AWA obtained from NIR were suitable methods for continuous moisture content measurement during fluid bed granulation. However, water balance measures the water amount in the entire process and thus water can in some cases be elsewhere than within the granules. Thus, differences between the in-line, on-line and off-line methods reflect the location of water in the process and its retention to different materials.

Dividing continuously recorded NIR spectra by the spectrum of the initial powder mixture produces curves that show only the spectral changes resulting from processing. The vast majority of these alterations are brought about by changes in particle size and moisture content. The data analysis approach applied in the study enabled continuous visualisation and monitoring of these changes.

The combination of on-line photometric imaging and near-infrared spectroscopy with continuous in-line process measurements enabled continuous evaluation of key product properties during fluid bed granulation and provided insight into batch performance.

The powder characterisation and PAT tools applied in this work enabled rapid and non-destructive determination of the key powder and granule quality attributes. Even small changes in the material properties during processing were detected using the continuous and complementary PAT tools. In the future, the simultaneous collection of image, NIR and process parameter information could help to improve the efficiency and robustness of especially continuous manufacturing processes.

References

Ahlneck, C. & Zografi, G. 1990. The molecular basis of moisture effects on the physical and chemical stability of drugs in the solid state. *Int. J. Pharm.,* 62**,** 87-95.

Alcala, M., Blanco, M., Bautista, M. & Gonzalez, J. M. 2010. On-line monitoring of a granulation process by nir spectroscopy. *J. Pharm. Sci.,* 99**,** 336-45.

Alkan, M. & Yuksel, A. 1986. Granulation in a fluidized bed ii effect of binder amount on the final granules. *Drug development and industrial pharmacy,* 12**,** 1529-1543.

Allen, T. 2003. *Powder sampling and particle size determination*, Elsevier.

Almeida-Prieto, S., Blanco-Méndez, J. & Otero-Espinar, F. J. 2006. Microscopic image analysis techniques for the morphological characterization of pharmaceutical particles: Influence of process variables. *Journal of pharmaceutical sciences,* 95**,** 348-357.

Andres, C., Réginault, P., Rochat, M., Chaillot, B. & Pourcelot, Y. 1996. Particle-size distribution of a powder: Comparison of three analytical techniques. *International journal of pharmaceutics,* 144**,** 141-146.

Antonyuk, S., Khanal, M., Tomas, J., Heinrich, S. & Mörl, L. 2006. Impact breakage of spherical granules: Experimental study and dem simulation. *Chemical Engineering and Processing: Process Intensification,* 45**,** 838-856.

Armstrong, N. 1997. Tableting. *Pharmaceutics: the science of dosage form design. 3rd Ed. Churchill Livingstone, New York*.

Bailey, A. 1984. Electrostatic phenomena during powder handling. *Powder Technology,* 37**,** 71-85.

Barnes, R., Dhanoa, M. & Lister, S. J. 1989. Standard normal variate transformation and de-trending of near-infrared diffuse reflectance spectra. *Appl. Spectmsc.,* 43**,** 772-777.

Berntsson, O., Danielsson, L. & Folestad, S. 1998. Estimation of effective sample size when analysing powders with diffuse reflectance near-infrared spectrometry. *Analytica chimica acta,* 364**,** 243-251.

Besenhard, M., Hohl, R., Hodzic, A., Eder, R. & Khinast, J. 2014. Modeling a seeded continuous crystallizer for the production of active pharmaceutical ingredients. *Crystal Research and Technology,* 49**,** 92-108.

Bika, D., Tardos, G., Panmai, S., Farber, L. & Michaels, J. 2005. Strength and morphology of solid bridges in dry granules of pharmaceutical powders. *Powder Technology,* 150**,** 104-116.

Blanco, M., Coello, J., Iturriaga, H., Maspoch, S. & Pagès, J. 1999. Calibration in non-linear near infrared reflectance spectroscopy: A comparison of several methods. *Anal. Chim. Acta,* 384**,** 207-214.

Blanco, M. & Villarroya, I. 2002. Nir spectroscopy: A rapid-response analytical tool. *TrAC, Trends Anal. Chem.,* 21**,** 240-250.

Bonifazi, G., La Marca, F. & Massacci, P. 2002. Characterization of bulk particles in real time. *Particle & Particle Systems Characterization,* 19**,** 240-246.

Bouffard, J., Kaster, M. & Dumont, H. 2005. Influence of process variable and physicochemical properties on the granulation mechanism of mannitol in a fluid bed top spray granulator. *Drug development and industrial pharmacy,* 31**,** 923-933.

Brunauer, S., Emmett, P. & Teller, E. 1938. Determined in our laboratory by bet method. *J. Am. Chem. Soc,* 60**,** 309.

Buckton, G., Yonemochi, E., Yoon, W. & Moffat, A. 1999. Water sorption and near ir spectroscopy to study the differences between microcrystalline cellulose and silicified microcrystalline cellulose before and after wet granulation. *Int. J. Pharm.,* 181**,** 41-47.

Burggraeve, A., Monteyne, T., Vervaet, C., Remon, J. P. & Beer, T. D. 2013. Process analytical tools for monitoring, understanding, and control of pharmaceutical fluidized bed granulation: A review. *Eur. J. Pharm. Biopharm.,* 83**,** 2-15.

Burggraeve, A., Sandler, N., Heinamaki, J., Raikkonen, H., Remon, J. P., Vervaet, C., De Beer, T. & Yliruusi, J. 2011a. Real-time image-based investigation of spheronization and drying phenomena using different pellet formulations. *Eur. J. Pharm. Sci.,* 44**,** 635-42.

Burggraeve, A., Silva, A. F., Van Den Kerkhof, T., Hellings, M., Vervaet, C., Paul Remon, J., Vander Heyden, Y. & De Beer, T. 2012. Development of a fluid bed granulation process control strategy based on real-time process and product measurements. *Talanta,* 100**,** 293-302.

Burggraeve, A., Van Den Kerkhof, T., Hellings, M., Remon, J. P., Vervaet, C. & De Beer, T. 2010. Evaluation of in-line spatial filter velocimetry as pat monitoring tool for particle growth during fluid bed granulation. *Eur. J. Pharm. Biopharm.,* 76**,** 138-46.

Burggraeve, A., Van den Kerkhof, T., Hellings, M., Remon, J. P., Vervaet, C. & De Beer, T. 2011b. Batch statistical process control of a fluid bed granulation process using in-line spatial filter velocimetry and product temperature measurements. *Eur. J. Pharm. Sci.,* 42**,** 584-592.

Burns, D. A. & Ciurczak, E. W. 2007. *Handbook of near-infrared analysis*, CRC press.

Buschmüller, C., Wiedey, W., Döscher, C., Dressler, J. & Breitkreutz, J. 2008. In-line monitoring of granule moisture in fluidized-bed dryers using microwave resonance technology. *Eur. J. Pharm. Biopharm.,* 69**,** 380-387.

Clydesdale, G., Roberts, K. J., Telfer, G. B. & Grant, D. J. 1997. Modeling the crystal morphology of α-lactose monohydrate. *J. Pharm. Sci.,* 86**,** 135-141.

Crouter, A. & Briens, L. 2014. The effect of moisture on the flowability of pharmaceutical excipients. *AAPS PharmSciTech,* 15**,** 65-74.

Crowder, T. M. & Hickey, A. J. 1999. An instrument for rapid powder flow measurement and temporal fractal analysis. *Particle & particle systems characterization,* 16**,** 32-34.

Davies, W. L. & Gloor, W. T. 1971. Batch production of pharmaceutical granulations in a fluidized bed i: Effects of process variables on physical properties of final granulation. *J. Pharm. Sci.,* 60**,** 1869-1874.

Davies, W. L. & Gloor, W. T. 1972. Batch production of pharmaceutical granulations in a fluidized bed ii: Effects of various binders and their concentrations on granulations and compressed tablets. *Journal of pharmaceutical sciences,* 61**,** 618-622.

Dawoodbhai, S. & Rhodes, C. T. 1989. The effect of moisture on powder flow and on compaction and physical stability of tablets. *Drug Dev. Ind. Pharm.,* 15**,** 1577-1600.

De Beer, T., Bodson, C., Dejaegher, B., Walczak, B., Vercruysse, P., Burggraeve, A., Lemos, A., Delattre, L., Heyden, Y. V. & Remon, J. P. 2008. Raman spectroscopy as a process analytical technology (pat) tool for the< i> in-line</i> monitoring and understanding of a powder blending process. *J. Pharm. Biomed. Anal.,* 48**,** 772-779.

De Beer, T., Burggraeve, A., Fonteyne, M., Saerens, L., Remon, J. P. & Vervaet, C. 2011. Near infrared and raman spectroscopy for the in-process monitoring of pharmaceutical production processes. *Int. J. Pharm.,* 417**,** 32-47.

Eggers, J., Kempkes, M. & Mazzotti, M. 2008. Measurement of size and shape distributions of particles through image analysis. *Chemical Engineering Science,* 63**,** 5513-5521.

Ek, R. & Newton, J. M. 1998. Microcrystalline cellulose as a sponge as an alternative concept to the crystallite-gel model for extrusion and spheronization. *Pharm. Res.,* 15**,** 509-512.

Ennis, B. & Litster, J. 1997. Particle size enlargement. *Perry's Chemical Engineers' Handbook, 7th edn, McGraw-Hill, New York***,** 20-56.

Faqih, A. M. N., Mehrotra, A., Hammond, S. V. & Muzzio, F. J. 2007. Effect of moisture and magnesium stearate concentration on flow properties of cohesive granular materials. *International journal of pharmaceutics,* 336**,** 338-345.

Faure, A., York, P. & Rowe, R. 2001. Process control and scale-up of pharmaceutical wet granulation processes: A review. *Eur. J. Pharm. Biopharm.,* 52**,** 269-277.
FDA 2004. Guidance for industry: Pat-a framework for innovative pharmaceutical development, manufacturing and quality assurance.
Fielden, K., Newton, J. M., O'BRIEN, P. & Rowe, R. C. 1988. Thermal studies on the interaction of water and microcrystalline cellulose. *J. Pharm. Pharmacol.,* 40**,** 674-678.
Findlay, W. P., Peck, G. R. & Morris, K. R. 2005. Determination of fluidized bed granulation end point using near-infrared spectroscopy and phenomenological analysis. *J. Pharm. Sci.,* 94**,** 604-12.
Fonteyne, M., Arruabarrena, J., de Beer, J., Hellings, M., Van Den Kerkhof, T., Burggraeve, A., Vervaet, C., Remon, J. P. & De Beer, T. 2014. Nir spectroscopic method for the in-line moisture assessment during drying in a six-segmented fluid bed dryer of a continuous tablet production line: Validation of quantifying abilities and uncertainty assessment. *J. Pharm. Biomed. Anal.,* 100C**,** 21-27.
Fonteyne, M., Soares, S., Vercruysse, J., Peeters, E., Burggraeve, A., Vervaet, C., Remon, J. P., Sandler, N. & De Beer, T. 2012. Prediction of quality attributes of continuously produced granules using complementary pat tools. *Eur. J. Pharm. Biopharm.,* 82**,** 429-436.
Frake, P., Greenhalgh, D., Grierson, S., Hempenstall, J. & Rudd, D. 1997. Process control and end-point determination of a fluid bed granulation by application of near infra-red spectroscopy. *Int. J. Pharm.,* 151**,** 75-80.
Gauthier, D., Zerguerras, S. & Flamant, G. 1999. Influence of the particle size distribution of powders on the velocities of minimum and complete fluidization. *Chemical Engineering Journal,* 74**,** 181-196.
Gradinarsky, L., Brage, H., Lagerholm, B., Björn, I. N. & Folestad, S. 2006. In situ monitoring and control of moisture content in pharmaceutical powder processes using an open-ended coaxial probe. *Measurement science and technology,* 17**,** 1847.
Grout, B. 2014. Application of near infrared conformance trending for material quality, container consistency and minimisation of process risk. *J. Near Infrared Spectrosc.,* 22**,** 169-178.
Gupta, A., Peck, G. E., Miller, R. W. & Morris, K. R. 2004. Nondestructive measurements of the compact strength and the particle-size distribution after milling of roller compacted powders by near-infrared spectroscopy. *J. Pharm. Sci.,* 93**,** 1047-1053.
Halenius, A., Lakio, S., Antikainen, O., Hatara, J. & Yliruusi, J. 2014. Fast tablet tensile strength prediction based on non-invasive analytics. *AAPS PharmSciTech,* 15**,** 781-791.
Halstensen, M., de Bakker, P. & Esbensen, K. H. 2006. Acoustic chemometric monitoring of an industrial granulation production process—a pat feasibility study. *Chemometrics and Intelligent Laboratory Systems,* 84**,** 88-97.
Halstensen, M. & Esbensen, K. 2000. New developments in acoustic chemometric prediction of particle size distribution—'the problem is the solution'. *Journal of chemometrics,* 14**,** 463-481.
Halstensen, M. & Esbensen, K. H. 2010. Acoustic chemometric monitoring of industrial production processes. *Process analytical technology***,** 281-302.
Hartung, A., Knoell, M., Schmidt, U. & Langguth, P. 2011. Role of continuous moisture profile monitoring by inline nir spectroscopy during fluid bed granulation of an enalapril formulation. *Drug Dev. Ind. Pharm.,* 37**,** 274-80.
Hassan, M. S. & Lau, R. W. M. 2009. Effect of particle shape on dry particle inhalation: Study of flowability, aerosolization, and deposition properties. *AAPS PharmSciTech,* 10**,** 1252-1262.
Hellén, L. & Yliruusi, J. 1993. Process variables of instant granulator and spheroniser: Iii. Shape and shape distributions of pellets. *International journal of pharmaceutics,* 96**,** 217-223.

Hellén, L., Yliruusi, J. & Kristoffersson, E. 1993. Process variables of instant granulator and spheroniser: Ii. Size and size distributions of pellets. *international Journal of Pharmaceutics,* 96**,** 205-216.
Hemati, M., Cherif, R., Saleh, K. & Pont, V. 2003. Fluidized bed coating and granulation: Influence of process-related variables and physicochemical properties on the growth kinetics. *Powder Technology,* 130**,** 18-34.
Hlinak, A. J., Kuriyan, K., Morris, K. R., Reklaitis, G. V. & Basu, P. K. 2006. Understanding critical material properties for solid dosage form design. *Journal of Pharmaceutical Innovation,* 1**,** 12-17.
Horn, B. K. 1970. Shape from shading: A method for obtaining the shape of a smooth opaque object from one view. *PhD Thesis, Massachusetts Institute of Technology*.
Horn, B. K. & Brooks, M. J. 1989. *Shape from shading*, MIT press.
Hu, X., Cunningham, J. C. & Winstead, D. 2008. Study growth kinetics in fluidized bed granulation with at-line fbrm. *Int. J. Pharm.,* 347**,** 54-61.
Huang, J. & Esbensen, K. H. 2000. Applications of angle measure technique (amt) in image analysis: Part i. A new methodology for in situ powder characterization. *Chemometrics and Intelligent Laboratory Systems,* 54**,** 1-19.
Iacocca, R. & German, R. 1997. A comparison of powder particle size measuring instruments. *International journal of powder metallurgy,* 33**,** 35-48.
ICH 2009. Guideline, pharmaceutical development. *Q8 (2R). As revised in August*.
Iveson, S. & Litster, J. 1998. Growth regime map for liquid-bound granules. *AIChE journal,* 44**,** 1510-1518.
Iveson, S. M., Litster, J. D., Hapgood, K. & Ennis, B. J. 2001. Nucleation, growth and breakage phenomena in agitated wet granulation processes: A review. *Powder Technol.,* 117**,** 3-39.
Jackson, J. E. 2005. *A user's guide to principal components*, John Wiley & Sons.
Jiang, Y., Matsusaka, S., Masuda, H. & Qian, Y. 2009. Development of measurement system for powder flowability based on vibrating capillary method. *Powder Technology,* 188**,** 242-247.
Juran, J. M. 1992. *Juran on quality by design: The new steps for planning quality into goods and services*, Simon and Schuster.
Juslin, L., Antikainen, O., Merkku, P. & Yliruusi, J. 1995a. Droplet size measurement: I. Effect of three independent variables on droplet size distribution and spray angle from a pneumatic nozzle. *International journal of pharmaceutics,* 123**,** 247-256.
Juslin, L., Antikainen, O., Merkku, P. & Yliruusi, J. 1995b. Droplet size measurement: Ii. Effect of three independent variables on parameters describing the droplet size distribution from a pneumatic nozzle studied by multilinear stepwise regression analysis. *International journal of pharmaceutics,* 123**,** 257-264.
Kadunc, N. O., Likar, B. & Tomaževič, D. 2014. In-line monitoring of pellet coating thickness growth by means of visual imaging. *Int. J. Pharm.,* 470**,** 8-14.
Karra, V. K. & Fuerstenau, D. 1977. The effect of humidity on the trace mixing kinetics in fine powders. *Powder Technology,* 16**,** 97-105.
Kempkes, M., Vetter, T. & Mazzotti, M. 2010. Measurement of 3d particle size distributions by stereoscopic imaging. *Chemical Engineering Science,* 65**,** 1362-1373.
Khanam, T., Nurur Rahman, M., Rajendran, A., Kariwala, V. & Asundi, A. K. 2011. Accurate size measurement of needle-shaped particles using digital holography. *Chemical Engineering Science,* 66**,** 2699-2706.
Kirsch, R. M., Williams, R. A., Bröckel, U., Hammond, R. B. & Jia, X. 2011. Direct observation of the dynamics of bridge formation between urea prills. *Industrial & Engineering Chemistry Research,* 50**,** 11728-11733.
Kontny, M. J. & Zografi, G. 1995. Sorption of water by solids. *Drugs and the Pharmaceutical Sciences,* 70**,** 387-387.
Krantz, M., Zhang, H. & Zhu, J. 2009. Characterization of powder flow: Static and dynamic testing. *Powder Technology,* 194**,** 239-245.
Labuza, T. 1968. Sorption phenomena in foods. *Food technology,* 22**,** 15-&.

Laitinen, N., Antikainen, O., Rantanen, J. & Yliruusi, J. 2004. New perspectives for visual characterization of pharmaceutical solids. *Journal of pharmaceutical sciences,* 93**,** 165-176.
Laitinen, N., Antikainen, O. & Yliruusi, J. 2002. Does a powder surface contain all necessary information for particle size distribution analysis? *European journal of pharmaceutical sciences,* 17**,** 217-227.
Laitinen, N., Antikainen, O. & Yliruusi, J. 2003. Characterization of particle sizes in bulk pharmaceutical solids using digital image information. *AAPS PharmSciTech,* 4**,** 383-391.
Lakio, S., Hatara, J., Tervakangas, H. & Sandler, N. 2012. Determination of segregation tendency of granules using surface imaging. *J. Pharm. Sci.,* 101**,** 2229-2238.
Lawrence, X. Y., Amidon, G., Khan, M. A., Hoag, S. W., Polli, J., Raju, G. & Woodcock, J. 2014. Understanding pharmaceutical quality by design. *The AAPS journal***,** 1-13.
Leskinen, J. T., Okkonen, M.-A. H., Toiviainen, M. M., Poutiainen, S., Tenhunen, M., Teppola, P., Lappalainen, R., Ketolainen, J. & Järvinen, K. 2010. Labscale fluidized bed granulator instrumented with non-invasive process monitoring devices. *Chemical Engineering Journal,* 164**,** 268-274.
Li, Q., Rudolph, V., Weigl, B. & Earl, A. 2004. Interparticle van der waals force in powder flowability and compactibility. *International journal of pharmaceutics,* 280**,** 77-93.
Liao, C. & Tarng, Y. 2009. On-line automatic optical inspection system for coarse particle size distribution. *Powder Technology,* 189**,** 508-513.
Lipps, D. M. & Sakr, A. M. 1994. Characterization of wet granulation process parameters using response surface methodology. 1. Top-spray fluidized bed. *Journal of pharmaceutical sciences,* 83**,** 937-947.
Lipsanen, T., Antikainen, O., Räikkönen, H., Airaksinen, S. & Yliruusi, J. 2007. Novel description of a design space for fluidised bed granulation. *Int. J. Pharm.,* 345**,** 101-107.
Liu, L., Marziano, I., Bentham, A., Litster, J., White, E. & Howes, T. 2008. Effect of particle properties on the flowability of ibuprofen powders. *International journal of pharmaceutics,* 362**,** 109-117.
Lourenço, V., Herdling, T., Reich, G., Menezes, J. C. & Lochmann, D. 2011. Combining microwave resonance technology to multivariate data analysis as a novel pat tool to improve process understanding in fluid bed granulation. *European Journal of Pharmaceutics and Biopharmaceutics,* 78**,** 513-521.
Lu, Z., Tai, Y.-W., Deng, F., Ben-Ezra, M. & Brown, M. S. 2013. A 3d imaging framework based on high-resolution photometric-stereo and low-resolution depth. *International journal of computer vision,* 102**,** 18-32.
Luypaert, J., Massart, D. & Vander Heyden, Y. 2007. Near-infrared spectroscopy applications in pharmaceutical analysis. *Talanta,* 72**,** 865-883.
Martin, K. A. 1993. Direct measurement of moisture in skin by nir spectroscopy. *Journal-society of cosmetic chemists,* 44**,** 249-249.
Matero, S., Den Berg, F. v., Poutiainen, S., Rantanen, J. & Pajander, J. 2013. Towards better process understanding: Chemometrics and multivariate measurements in manufacturing of solid dosage forms. *Journal of pharmaceutical sciences,* 102**,** 1385-1403.
Matero, S., Poutiainen, S., Leskinen, J., Järvinen, K., Ketolainen, J., Poso, A. & Reinikainen, S. P. 2010. Estimation of granule size distribution for batch fluidized bed granulation process using acoustic emission and n-way pls. *Journal of Chemometrics,* 24**,** 464-471.
Matero, S., Poutiainen, S., Leskinen, J., Järvinen, K., Ketolainen, J., Reinikainen, S. P., Hakulinen, M., Lappalainen, R. & Poso, A. 2009. The feasibility of using acoustic emissions for monitoring of fluidized bed granulation. *Chemometrics and Intelligent Laboratory Systems,* 97**,** 75-81.

Merkku, P., Antikainen, O. & Yliruusi, J. 1993. Use of 33 factorial design and multilinear stepwise regression analysis in studying the fluidized bed granulation process. Ii. *European journal of pharmaceutics and biopharmaceutics,* 39**,** 112-116.

Murtomaa, M. & Laine, E. 2000. Electrostatic measurements on lactose–glucose mixtures. *Journal of Electrostatics,* 48**,** 155-162.

Närvänen, T., Lipsanen, T., Antikainen, O., Räikkönen, H., Heinämäki, J. & Yliruusi, J. 2009. Gaining fluid bed process understanding by in-line particle size analysis. *Journal of pharmaceutical sciences,* 98**,** 1110-1117.

Närvänen, T., Seppälä, K., Antikainen, O. & Yliruusi, J. 2008. A new rapid on-line imaging method to determine particle size distribution of granules. *AAPS PharmSciTech,* 9**,** 282-287.

Nieuwmeyer, F. J., Damen, M., Gerich, A., Rusmini, F., van der Voort Maarschalk, K. & Vromans, H. 2007a. Granule characterization during fluid bed drying by development of a near infrared method to determine water content and median granule size. *Pharm. Res.,* 24**,** 1854-61.

Nieuwmeyer, F. J., van der Voort Maarschalk, K. & Vromans, H. 2007b. Granule breakage during drying processes. *Int. J. Pharm.,* 329**,** 81-7.

Osborne, B. G., Douglas, S. & Fearn, T. 1981. Assessment of wheat grain texture by near infrared reflectance measurements on bühler-milled flour. *Journal of the Science of Food and Agriculture,* 32**,** 200-202.

Otsuka, M., Koyama, A. & Hattori, Y. 2014. Real-time release monitoring for water content and mean particle size of granules in lab-sized fluid-bed granulator by near-infrared spectroscopy. *RSC Advances,* 4**,** 17461-17468.

Parikh, D. M. 2009. *Handbook of pharmaceutical granulation technology, 3rd ed*, CRC Press.

Patchigolla, K. & Wilkinson, D. 2009. Crystal shape characterisation of dry samples using microscopic and dynamic image analysis. *Particle & Particle Systems Characterization,* 26**,** 171-178.

Peinado, A., Hammond, J. & Scott, A. 2011. Development, validation and transfer of a near infrared method to determine in-line the end point of a fluidised drying process for commercial production batches of an approved oral solid dose pharmaceutical product. *J. Pharm. Biomed. Anal.,* 54**,** 13-20.

Petrak, D. 2002. Simultaneous measurement of particle size and particle velocity by the spatial filtering technique. *Particle & Particle Systems Characterization,* 19**,** 391-400.

Pons, M., Vivier, H., Belaroui, K., Bernard-Michel, B., Cordier, F., Oulhana, D. & Dodds, J. 1999. Particle morphology: From visualisation to measurement. *Powder Technology,* 103**,** 44-57.

Rajalahti, T. & Kvalheim, O. M. 2011. Multivariate data analysis in pharmaceutics: A tutorial review. *Int. J. Pharm.,* 417**,** 280-290.

Rambali, B., Baert, L. & Massart, D. 2001. Using experimental design to optimize the process parameters in fluidized bed granulation on a semi-full scale. *International journal of pharmaceutics,* 220**,** 149-160.

Rantanen, J., Jørgensen, A., Räsänen, E., Luukkonen, P., Airaksinen, S., Raiman, J., Hänninen, K., Antikainen, O. & Yliruusi, J. 2001a. Process analysis of fluidized bed granulation. *AAPS PharmSciTech,* 2**,** 13-20.

Rantanen, J., Känsäkoski, M., Suhonen, J., Tenhunen, J., Lehtonen, S., Rajalahti, T., Mannermaa, J.-P. & Yliruusi, J. 2000. Next generation fluidized bed granulator automation. *AAPS PharmSciTech,* 1**,** 26-36.

Rantanen, J., Räsänen, E., Antikainen, O., Mannermaa, J.-P. & Yliruusi, J. 2001b. In-line moisture measurement during granulation with a four-wavelength near-infrared sensor: An evaluation of process-related variables and a development of non-linear calibration model. *Chemometrics and Intelligent Laboratory Systems,* 56**,** 51-58.

Räsänen, E., Rantanen, J., Mannermaa, J. P. & Yliruusi, J. 2004. The characterization of fluidization behavior using a novel multichamber microscale fluid bed. *Journal of pharmaceutical sciences,* 93**,** 780-791.

Reich, G. 2005. Near-infrared spectroscopy and imaging: Basic principles and pharmaceutical applications. *Adv Drug Deliv Rev,* 57**,** 1109-43.
Rinnan, Å., van den Berg, F. & Engelsen, S. B. 2009. Review of the most common pre-processing techniques for near-infrared spectra. *TrAC, Trends Anal. Chem.,* 28**,** 1201-1222.
Roggo, Y., Chalus, P., Maurer, L., Lema-Martinez, C., Edmond, A. & Jent, N. 2007. A review of near infrared spectroscopy and chemometrics in pharmaceutical technologies. *J. Pharm. Biomed. Anal.,* 44**,** 683-700.
Rohera, B. D. & Zahir, A. 1993. Granulations in a fluidized-bed: Effect of binders and their concentrations on granule growth and modeling the relationship between granule size and binder concentration. *Drug development and industrial pharmacy,* 19**,** 773-792.
Rosas, J. G., de Waard, H., De Beer, T., Vervaet, C., Remon, J. P., Hinrichs, W. L., Frijlink, H. W. & Blanco, M. 2014. Nir spectroscopy for the in-line monitoring of a multicomponent formulation during the entire freeze-drying process. *J. Pharm. Biomed. Anal.,* 97**,** 39-46.
Ruppel, J., Müller, A.-K., Althaus, G., Drexel, C.-P. & Zimmermann, I. 2009. The modified outflow funnel—a device to assess the flow characteristics of powders. *Powder Technology,* 193**,** 87-92.
Russ, J. C. 2010. *The image processing handbook*, CRC press.
Saerens, L., Vervaet, C., Remon, J. P. & De Beer, T. 2014. Process monitoring and visualization solutions for hot-melt extrusion: A review. *J. Pharm. Pharmacol.,* 66**,** 180-203.
Sandler, N. 2011. Photometric imaging in particle size measurement and surface visualization. *Int. J. Pharm.,* 417**,** 227-34.
Sandler, N. & Wilson, D. 2010. Prediction of granule packing and flow behavior based on particle size and shape analysis. *Journal of pharmaceutical sciences,* 99**,** 958-968.
Schaafsma, S., Vonk, P. & Kossen, N. 2000. Fluid bed agglomeration with a narrow droplet size distribution. *Int. J. Pharm.,* 193**,** 175-187.
Schaafsma, S. H., Kossen, N. W., Mos, M. T., Blauw, L. & Hoffmann, A. C. 1999. Effects and control of humidity and particle mixing in fluid-bed granulation. *AIChE J.,* 45**,** 1202-1210.
Schaafsma, S. H., Vonk, P., Segers, P. & Kossen, N. W. 1998. Description of agglomerate growth. *Powder Technol.,* 97**,** 183-190.
Schaefer, T. 1988. Equipment for wet granulation. *Acta Pharmaceutica Suecica,* 25**,** 205-228.
Schaefer, T. & Worts, O. 1977. Control of fluidized bed granulation. I. Effects of spray angle, nozzle height and starting materials on granule size and size distribution. *Arch Pharm Chem Sci,* 5**,** 51-60.
Schaefer, T. & Wørts, O. 1978. Control of fluidized bed granulation iv. Effects of binder solution and atomization on granule size and size distribution. *Arch Pharm Chem Sci,* 6**,** 14-25.
Scharstein, D. & Szeliski, R. 2002. A taxonomy and evaluation of dense two-frame stereo correspondence algorithms. *International journal of computer vision,* 47**,** 7-42.
Scharstein, D. & Szeliski, R. High-accuracy stereo depth maps using structured light. Computer Vision and Pattern Recognition, 2003. Proceedings. 2003 IEEE Computer Society Conference on, 2003. IEEE, I-195-I-202 vol. 1.
Schinzinger, O. & Schmidt, P. C. 2005. Comparison of the granulation behavior of three different excipients in a laboratory fluidized bed granulator using statistical methods. *Pharmaceutical development and technology,* 10**,** 175-188.
Seitz, S. M., Curless, B., Diebel, J., Scharstein, D. & Szeliski, R. A comparison and evaluation of multi-view stereo reconstruction algorithms. Computer vision and pattern recognition, 2006 IEEE Computer Society Conference on, 2006. IEEE, 519-528.

Shekunov, B. Y., Chattopadhyay, P., Tong, H. H. & Chow, A. H. 2007. Particle size analysis in pharmaceutics: Principles, methods and applications. *Pharmaceutical research,* 24**,** 203-227.
Shi, Z. & Anderson, C. A. 2010. Application of monte carlo simulation-based photon migration for enhanced understanding of near-infrared (nir) diffuse reflectance. Part i: Depth of penetration in pharmaceutical materials. *Journal of pharmaceutical sciences,* 99**,** 2399-2412.
Shiraishi, T., Sano, A., Kondo, S., Yuasa, H. & Kanaya, Y. 1995. Studies on the granulation process of granules for tableting with a high speed mixer. Ii: Influence of particle size of active substance on granulation. *Chemical and pharmaceutical bulletin,* 43**,** 654-659.
Siesler, H. W., Ozaki, Y., Kawata, S. & Heise, H. M. 2008. *Near-infrared spectroscopy: Principles, instruments, applications*, John Wiley & Sons.
Silva, A. F., Burggraeve, A., Denon, Q., Van der Meeren, P., Sandler, N., Van Den Kerkhof, T., Hellings, M., Vervaet, C., Remon, J. P. & Lopes, J. A. 2013. Particle sizing measurements in pharmaceutical applications: Comparison of in-process methods versus off-line methods. *Eur. J. Pharm. Biopharm.,* 85**,** 1006-1018.
Staniforth, J. 2007. Powder flow in: Aulton's pharmaceutics: The design and manufacturing of medicines, 3rd ed. Hungary: Harcourt publisher ltd.
Sun, C. & Grant, D. J. 2001. Effects of initial particle size on the tableting properties of l-lysine monohydrochloride dihydrate powder. *International Journal of pharmaceutics,* 215**,** 221-228.
Swaminathan, V. & Kildsig, D. O. 2002. Polydisperse powder mixtures: Effect of particle size and shape on mixture stability. *Drug development and industrial pharmacy,* 28**,** 41-48.
Teunou, E., Fitzpatrick, J. & Synnott, E. 1999. Characterisation of food powder flowability. *Journal of Food Engineering,* 39**,** 31-37.
Ticehurst, M., York, P., Rowe, R. & Dwivedi, S. 1996. Characterisation of the surface properties of α-lactose monohydrate with inverse gas chromatography, used to detect batch variation. *Int. J. Pharm.,* 141**,** 93-99.
Tok, A. T., Goh, X., Ng, W. K. & Tan, R. B. 2008. Monitoring granulation rate processes using three pat tools in a pilot-scale fluidized bed. *AAPS PharmSciTech,* 9**,** 1083-91.
Treffer, D., Wahl, P. R., Hörmann, T. R., Markl, D., Schrank, S., Jones, I., Cruise, P., Mürb, R.-K., Koscher, G. & Roblegg, E. 2014. In-line implementation of an image-based particle size measurement tool to monitor hot-melt extruded pellets. *Int. J. Pharm.,* 466**,** 181-189.
Tsujimoto, H., Yokoyama, T., Huang, C. & Sekiguchi, I. 2000. Monitoring particle fluidization in a fluidized bed granulator with an acoustic emission sensor. *Powder technology,* 113**,** 88-96.
Van Veen, B., Pajander, J., Zuurman, K., Lappalainen, R., Poso, A., Frijlink, H. & Ketolainen, J. 2005. The effect of powder blend and tablet structure on drug release mechanisms of hydrophobic starch acetate matrix tablets. *European journal of pharmaceutics and biopharmaceutics,* 61**,** 149-157.
Vanarase, A. U., Alcala, M., Jerez Rozo, J. I., Muzzio, F. J. & Romañach, R. J. 2010. Real-time monitoring of drug concentration in a continuous powder mixing process using nir spectroscopy. *Chemical Engineering Science,* 65**,** 5728-5733.
Visser, J. 1989. Van der waals and other cohesive forces affecting powder fluidization. *Powder Technology,* 58**,** 1-10.
Vogiatzis, G. & Hernández, C. 2010. Practical 3d reconstruction based on photometric stereo. *Computer vision.* Springer.
Wahl, P. R., Fruhmann, G., Sacher, S., Straka, G., Sowinski, S. & Khinast, J. G. 2014. Pat for tableting: Inline monitoring of api and excipients via nir spectroscopy. *Eur. J. Pharm. Biopharm.*

Wang, X. Z., Roberts, K. J. & Ma, C. 2008. Crystal growth measurement using 2d and 3d imaging and the perspectives for shape control. *Chemical Engineering Science,* 63**,** 1173-1184.
Ward, H. W., Blackwood, D. O., Polizzi, M. & Clarke, H. 2013. Monitoring blend potency in a tablet press feed frame using near infrared spectroscopy. *Journal of pharmaceutical and biomedical analysis,* 80**,** 18-23.
Watano, S. 2001. Direct control of wet granulation processes by image processing system. *Powder technology,* 117**,** 163-172.
Watano, S. & Miyanami, K. 1995. Image processing for on-line monitoring of granule size distribution and shape in fluidized bed granulation. *Powder technology,* 83**,** 55-60.
Watano, S., Sato, Y. & Miyanami, K. 1996. Control of granule growth in fluidized bed granulation by an image processing system. *Chemical and pharmaceutical bulletin,* 44**,** 1556-1560.
Watano, S., Sato, Y. & Miyanami, K. 1997. Optimization and validation of an image processing system in fluidized bed granulation. *Advanced Powder Technology,* 8**,** 269-277.
Wildfong, P. L., Samy, A. S., Corfa, J., Peck, G. E. & Morris, K. R. 2002. Accelerated fluid bed drying using nir monitoring and phenomenological modeling: Method assessment and formulation suitability. *J. Pharm. Sci.,* 91**,** 631-639.
Wöhler, C. 2013. *3d computer vision, 2nd ed*, Springer.
Wold, S., Sjöström, M. & Eriksson, L. 2001. Pls-regression: A basic tool of chemometrics. *Chemometrics and intelligent laboratory systems,* 58**,** 109-130.
Woodham, R. J. 1980. Photometric method for determining surface orientation from multiple images. *Optical engineering,* 19**,** 191139-191139-.
Wørts, O. 1998. Wet granulation—fluidized bed and high shear techniques compared. *Pharm. Technol. Eur,* 10**,** 27-30.
Yajima, T., Itai, S., Hayashi, H., Takayama, K. & Nagai, T. 1996. Optimization of size distribution of granules for tablet compression. *Chemical and pharmaceutical bulletin,* 44**,** 1056-1060.
Yu, C., Xu, Y. & Wang, X. 1998. Study of fluidized-bed spray granulation. *Drying technology,* 17**,** 1893-1904.
Yu, W. & Hancock, B. C. 2008. Evaluation of dynamic image analysis for characterizing pharmaceutical excipient particles. *International journal of pharmaceutics,* 361**,** 150-157.
Zeng, X. M., Martin, G. P., Marriott, C. & Pritchard, J. 2000. The influence of carrier morphology on drug delivery by dry powder inhalers. *International journal of pharmaceutics,* 200**,** 93-106.
Zografi, G. 1988. States of water associated with solids. *Drug Dev. Ind. Pharm.,* 14**,** 1905-1926.
Zografi, G., Kontny, M., Yang, A. & Brenner, G. 1984. Surface area and water vapor sorption of macrocrystalline cellulose. *Int. J. Pharm.,* 18**,** 99-116.
Zografi, G. & Kontny, M. J. 1986. The interactions of water with cellulose-and starch-derived pharmaceutical excipients. *Pharm. Res.,* 3**,** 187-194.